A STUDY OF THE MEAN-SQUARE DISPLACEMENT AMPLITUDES OF T AND O ATOMS IN FRAMEWORK SILICATES AND ALUMINOSILICATES: EVIDENCE FOR RIGID TO BONDS, ORDER, DISORDER, TWINNING AND STACKING FAULTS IN CRYSTALS

by

Robert T. Downs

Thesis submitted to the Faculty of the
Virginia Polytechnic Institute and State University
in partial fulfillment of the requirements for the degree of
MASTER OF SCIENCE
in
Geological Sciences

APPROVED:

G.V. Gibbs, Co-Chairman

M.B. Boisen, Jr., Co-Chairman

P.H. Ribbe

J.C. Schug

M.E. Davis

December, 1989

Blacksburg, Virginia

A STUDY OF THE MEAN-SQUARE DISPLACEMENT AMPLITUDES OF T AND O ATOMS IN FRAMEWORK SILICATES AND ALUMINOSILICATES: EVIDENCE FOR RIGID TO BONDS, ORDER, DISORDER, TWINNING AND STACKING FAULTS IN CRYSTALS

by

Robert T. Downs

G.V. Gibbs and M.B. Boisen, Jr., Co-Chairmen

Geological Sciences

(ABSTRACT)

The mean-square displacement amplitudes (MSDA) of the tetrahedral cations Si and Al are compared to the MSDA of their coordinated O atoms in framework silica polymorphs and aluminosilicate structures. Criteria are established which indicate order, structural disorder or substitutional disorder in a framework crystal.

ACKNOWLEDGEMENTS

I wish to thank my committee members for all their suggestions and good advice, especially and . Special thanks goes to my best friends and without whom life in Blacksburg would truly be bleak. Also, who convinced me to go to graduate school. The National Science Foundation supported this effort with Grant EAR-8803933 awarded to GVG and MBB for studying mathematical modelling of silicates.

TABLE OF CONTENTS

Abstract.....ii

Acknowledgements.....iii

Introduction.....1

Appendix.....31

References.....51

Vita.....60

INTRODUCTION

An examination of the isotropic displacement factors of the O atoms, B(O), recorded for framework silicates shows that two distinct populations can be defined, one with B(O)-values concentrated in the range between 0.25 and 3.0Å^2 and the other with B(O)-values spread rather uniformly between 4.5 and 10.0Å^2 (Boisen *et al.*, 1990). A stepwise regression analysis of the apparent SiO bond length data, R(SiO), for the silicates comprising the first population indicates that R(SiO) correlates with B(O), with the fraction of *s*-character of O and Si, f_S(O), f_S(Si), respectively, and with P, the pressure at which the diffraction data were recorded. A similar regression analysis of the bond length data for the second population indicates that R(SiO) correlates only with B(O), the other parameters failing to make a significant contribution to the regression sum of squares (See also Liebau, 1985). Following proposals by Liebau (1985) and others, it has been concluded that the silicates comprising the bulk of the second population probably exhibit some form of static disorder. The data comprising this population was obtained for the clathrasils and several tridymite crystals. As observed by Gies (1983; 1984; 1986) and Kihara (1978), these substances are typically twinned, a feature that has been ascribed to the presence of stacking faults of layers of silicate tetrahedra (Flörke, 1954; 1955). Boisen *et al.*, (1990) have argued that these stacking faults may account in part for the larger B(O)-values recorded for the crystals comprising this population.

In this paper, the mean-square displacement amplitudes, MSDA's, of the Si and O atoms are calculated in the direction of the SiO bonds for the framework silicates coesite, quartz and low cristobalite, using the anisotropic Gaussian displacement parameters recorded in structural analyses of these minerals. Similar calculations are presented for clathrasil and tridymite crystals and a variety of

aluminosilicates framework structures. A study of the MSDA's will suggest that the TO bonds (T=Si,Al) in the framework silicates and a number of ordered aluminosilicate structures behave as rigid bonds with the T and O atoms vibrating along the bonds in tandem. Criteria based on these MSDA data will be presented for testing a structure for substitutional disorder, twinning and stacking faults. The paper concludes with an examination of the factors that may affect the orientations of the displacement ellipsoids of the O atoms in ordered and disordered silicate and aluminosilicate framework structures.

Mean-Square Displacement Amplitudes and Evidence for Order, Disorder, Twinning and Stacking Faults in Crystals

If the AB bonds between atoms A and B comprising an AB_n-coordinated polyhedron in a crystal are rigid, then one would expect that the atoms should appear to vibrate in tandem and so the MSDA of A toward B, z^2_{AB}, and that of B toward A, z^2_{BA}, should tend to be nearly equal (Hirshfeld, 1976; Dunitz *et al.*, 1988). Moreover, if the displacement parameters of A and B define anisotropic ellipsoids, then z^2_{AB} and z^2_{BA} should be linearly correlated. This correlation will be enhanced if the AB bonds are measured at a variety of temperatures. The extent to which the correlation is developed should also depend on the extent to which the MSDA's depend on the static (substitutional and positional disorder, twinning and stacking faults) and the dynamic disorder (thermal and zero-point motion) exhibited by the atoms in the crystal. The MSDA's may also depend on the charge density deformation ascribed to the formation of chemical bonds (Hirshfeld, 1976). As the equivalent isotropic displacement factors recorded in a monopole refinement of the charge density for coesite are only about 5% larger than those recorded in a refinement with higher multipoles (Geisinger *et al.*, 1987), we will assume that

the charge density deformation in coesite and the other silicates examined in this study will have a relatively small effect on the MSDA's and therefore can be ignored.

If atoms A and B, comprising an AB bond exhibit anisotropic displacements and vibrate in tandem as a rigid bond, and if the components of static disorder are minimal, then the MSDA's for a series of crystals containing AB bonds should be linearly correlated with slope 1.0 and intercept 0.0. On the other hand, if the component of static disorder is significant, then the correlation between z^2_{AB} and z^2_{BA} should be less well-developed. With this reasoning, if the framework silicates comprising the first population defined by Boisen *et al.* (1990) lack a significant component of static disorder, if the Si and O atoms in these crystals vibrate in tandem as a rigid bond, then z^2_{SiO} should be highly correlated with z^2_{OSi}, particularly since their diffraction data were recorded at temperatures of 15K, room temperature and 480K. On the other hand, if the clathrasils and the low tridymite crystals that comprise the second population contain a significant component of static disorder, as argued by Liebau (1984), then z^2_{SiO} should be largely independent, on average, of z^2_{OSi}.

The Mean-Square Displacement Amplitudes for Si and O along the SiO bonds of the Framework Silicates

In this paper, we did not use all of the data used by Boisen *et al.* (1990) to construct their two populations because a number of those data were obtained from refinements completed with an isotropic displacement factor model. Instead, we used only the data for which anisotropic refinements have been completed at room pressure. Thus, the first population examined in our study consists of 96 R(SiO) bond length data recorded for coesite (Gibbs *et al.*, 1977; Levien

and Prewitt, 1981; Kirfel and Will, 1984; Smyth *et al.*, 1987; Geisinger *et al.*, 1987), low-cristobalite (Peacor, 1973), low-quartz (Young and Post, 1962; LePage and Donnay, 1976; Levien *et al.*, 1980; Wright and Lehmann, 1981), and high-quartz (Wright and Lehmann, 1981), structures which have B(O)-values ≤ 3.0Å^2. The second population examined by us consists of 181 R(SiO) data recorded in several studies of clathrate (Gies, 1983, 1984, 1986; Gerke and Gies, 1984) and tridymite crystals (Dollase, 1967; Kihara, 1977, 1978; Kihara *et al.*, 1986a, 1986b), structures which have B(O)-values greater than 4.0Å^2.

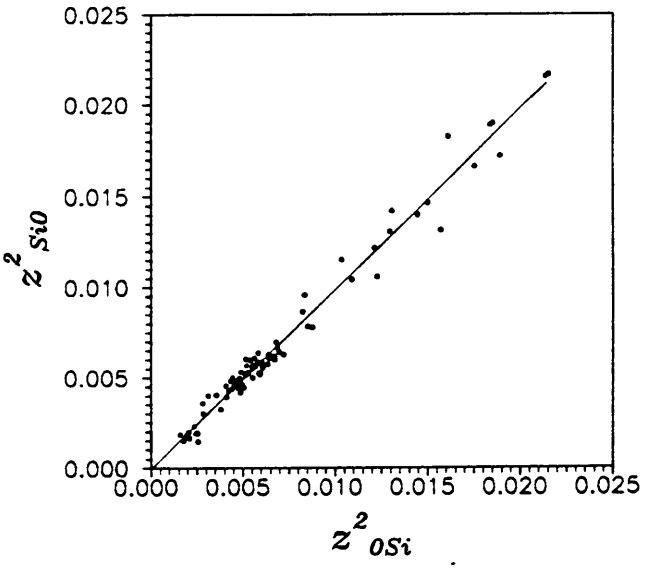

Figure 1. z^2_{SiO} vs. z^2_{OSi} for the framework silicates coesite, quartz and cristobalite. The regression equation is $z^2_{SiO} = -0.00006 + 0.992 z^2_{OSi}$ where $\sigma(-0.00006) = 0.00012$Å^2, $\sigma(0.992) = 0.015$ and the coefficient of determination is $r^2 = 0.98$.

The software METRIC (Boisen *et al.*, 1990) was used to calculate z^2_{SiO} and z^2_{OSi} from the ADP's recorded for each Si and O atom comprising the SiO bonds of the two populations. Figure 1 is a scatter diagram of z^2_{SiO} vs. z^2_{OSi} calculated from the first population. The slope of the regression line for this data is 0.99, the intercept is -0.00006Å^2 and the coefficient of determination is $r^2 = 0.98$. As

the estimated slope and intercept are not significantly different from 1.0 and 0.0, we conclude that the MSDA's measured for the Si and O atoms of quartz, coesite and cristobalite conform with a trend expected for a set of SiO bonds behaving as rigid units. We also conclude that the ADP's recorded for these minerals probably provide a reasonable measure of the dynamic disorder of the Si and O atoms in these crystals. It is noteworthy that a calculation of $\Delta = z^2_{OSi} - z^2_{SiO}$ for these minerals shows a maximum deviation from zero of $\pm 0.0015 \text{Å}^2$, which conforms with that ($\pm 0.001 \text{Å}^2$) proposed for the rigid, covalent CC bonds in several molecular crystals (Hirshfeld, 1976), with that ($\pm 0.0007 \text{Å}^2$) measured for the SiO bonds of the monopolysilicate anions in enstatite (Ghose *et al.*, 1986), but somewhat smaller than that ($\pm 0.003 \text{Å}^2$) recorded for the more ionic metal-ligand bonds in a variety of transition-metal complexes (Bürgi, 1984).

A scatter diagram of z^2_{SiO} vs. z^2_{OSi} prepared for the O and Si atoms comprising the crystals of the second population shows a relatively wide scatter of points (See Figure 2).

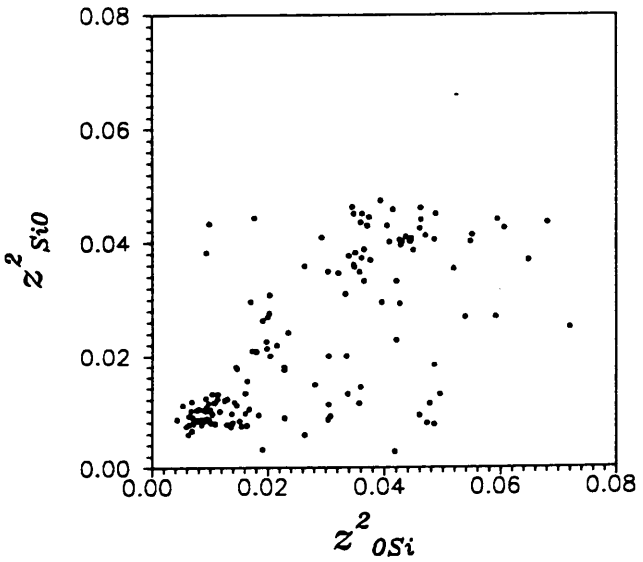

Figure 2. z^2_{SiO} vs. z^2_{OSi} for the clathrates and tridymites.

Hence, we conclude that the ADP's measured for these minerals describe a significant component of static disorder. Considering the relatively wide scatter of these points, it appears that a significant fraction of the atoms in the clathrates and the low tridymites are probably displaced from the positions that they would occupy in domains that are free of stacking faults. A refinement of a set of diffraction data recorded for such crystals should yield a set of positional parameters and ADP's that are affected by such defects. For example, the B-values recorded for both Si and O should be significantly larger and the apparent bond lengths calculated from the positional parameters should be significantly shorter than those recorded for quartz, coesite and cristobalite. This also implies that R(SiO) should correlate with both B(O) and B(Si) for this population. Individual linear regression analyses of R(SiO) as a function of each of the variables B(O), B(Si), f_s(O) and f_s(Si) shows that B(O) and B(Si) are the most highly correlated with R(SiO) (Boisen *et al.*, 1990). However, when all of these variables are included in a stepwise regression analysis, only B(O) makes a significant contribution to the sum of squares. As mentioned above, this may explains why the R(SiO)-values observed for the clathrasils and low tridymites are significantly shorter than those recorded for quartz, cristobalite and coesite (Liebau, 1985).

The Mean-Square Displacements Along the TO Bonds of Ordered and Disordered Alkali Feldspars

The structure of a feldspar mineral consists of a framework of corner sharing TO_4 tetrahedra (T = Al,Si) with either monovalent and or divalent cations tucked into the available cavities to neutralize the overall charge of the framework. As is well known, the alkali feldspars are believed to exhibit a variety of structural states ranging from a disordered state, in which the Al and Si atoms are randomly

distributed among all of the TO_4 groups, to a configuration in which these atoms are ordered into an array of translationally equivalent TO_4 groups. As shown by Smith (1954) and Smith and Bailey (1963), the mean TO bond length, $\langle$R(TO)$\rangle$ for a given TO_4 group in feldspar varies linearly with Al content from 1.61Å for a TO_4 group containing only Si to 1.74Å for a group containing only Al. As the alkali feldspars are believed to exhibit a continuum of intermediate structural states ranging between ordered and disordered configurations, we have an opportunity to examine how z^2_{TO}, z^2_{OT} and $\Delta = z^2_{OT} - z^2_{TO}$ vary with structural state. We also have an opportunity to examine how z^2_{TO} vs. z^2_{OT} scatter diagrams for structures that exhibit substitutional disorder compare with those obtained for structures that exhibit disorder ascribed to stacking faults and twinning.

Bürgi (1989) has published a scatter diagram prepared by Kunz and Armbruster (1990) for both ordered and disordered alkali feldspars, of the average value of Δ, $\langle\Delta\rangle$, for 138 individual TO_4 tetrahedra vs. $\langle$R(TO)$\rangle$ and has found that $\langle\Delta\rangle$ varies as a quadratic function of $\langle$R(TO)$\rangle$ according to the theoretical equation

$$\langle\Delta_t\rangle = (1.744 - \langle\mathrm{R(TO)}\rangle) \times (\langle\mathrm{R(TO)}\rangle - 1.607). \qquad (1)$$

An examination of this diagram shows that $\langle\Delta\rangle$ is smallest (± 0.0015Å^2) for the Al- and Si-rich tetrahedra in the ordered feldspars low albite and low microcline while it is as large as ± 0.007Å^2 for the disordered and partly ordered tetrahedra in intermediate albite and microcline, orthoclase, high albite and sanidine. The $\langle\Delta\rangle$-values obtained for the Si- and Al-rich tetrahedra are in exact agreement with those obtained above for the silicate tetrahedra of the framework silicates.

As low albite and low microcline both are believed to contain an ordered array of Al- and Si-rich tetrahedra, we plotted z^2_{TO} vs. z^2_{OT} for the 160 TO bonds for the tetrahedra of these feldspars in Figure 3 to learn how such a plot compares with

the one prepared for quartz, coesite and cristobalite. The data used to prepare this plot were taken from Winter *et al.* (1977); Harlow and Brown (1980); Strob (1981); Blasi *et al.* (1984); Smith *et al.* (1986); Blasi *et al.* (1987) and Armbruster *et al.* (1990). As these data were collected over a wide range of temperatures from 13K to 1243K, the range of the MSDA-values recorded for this data set is significantly larger, as expected, than that recorded for the framework silicates, which were collected over a smaller temperature range between 15K and 480K.

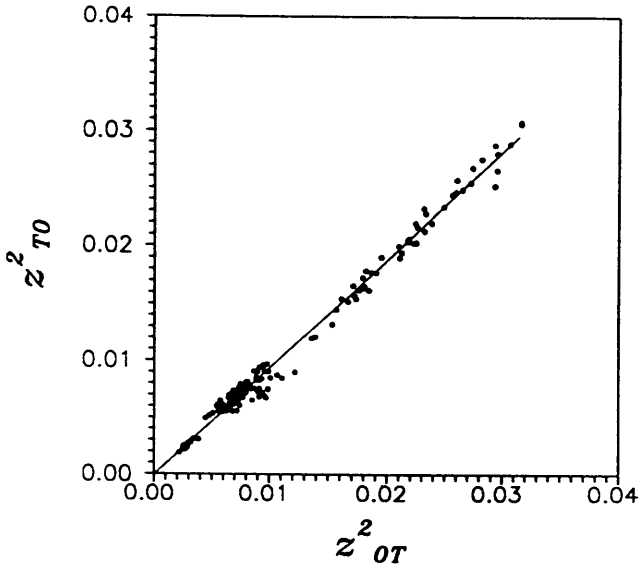

Figure 3. z^2_{TO} vs. z^2_{OT} for low albite and low microcline. The regression equation is $z^2_{SiO} = -0.00008 + 0.940 z^2_{OSi}$ where $\sigma(-0.00008) = 0.00011\text{Å}^2$, $\sigma(0.940) = 0.008$ and the coefficient of determination is $r^2 = 0.99$.

A linear regression analysis of the data used to prepare Figure 3 yields a slope of 0.94, an intercept of -0.00008Å^2 and a coefficient of determination of $r^2 = 0.99$. As the slope of the regression line departs from the ideal 45° line by only 1.8°, we conclude that these data are consistent with the Megaw (1974) view of the feldspar structure as an engineering construct of rigid rods connected together with TOT angle-brackets "made of springy material." Also, because the

$\langle\Delta\rangle$-values measured for these feldspars match those measured for quartz, coesite and cristobalite, we conclude that the component of substitutional disorder in low albite and low microcline is probably very small, if not absent. Although the intercept of the line calculated for these feldspars is not significantly different from 0.0, we note that the slope of the line is indeed significantly less than the ideal value of 1.0. This indicates that z^2_{OT} tends to increase at a somewhat faster rate than z^2_{TO} unlike the framework silicates where both of these parameters appear to increase at about the same rate.

The Al and Si atoms in the alkali feldspars, high albite and sanidine, are believed to be completely disordered over the TO_4 tetrahedra of the structures on the basis of their mean TO bond lengths. A plot of z^2_{TO} vs. z^2_{OT} for the TO bonds of these feldspars was prepared (Figure 4) to learn how such a plot compares with the one prepared for the clathrasils and the tridymites, on the one hand, and with the one for low albite and low microcline, on the other. The 162 data used to prepare the figure were taken from refinements by Weitz (1972), Phillips and Ribbe (1973), Keefer and Brown (1978), Winter *et al.*(1979), Blasi *et al.*(1981) and Scambos *et al.*(1987). The data in this plot scatter in a relatively wide linear band with a r^2 of 0.92. The cluster of points in the figure at the bottom right of the line, which seem to depart from the trend of the remaining data, are from a heated and unheated Eifel sanidine refined at room temperature by Weitz (1972). An explanation for the departure of this data from the line will be offered later. All the data were chosen from structure refinements of crystals that were considered to be completely disordered.

A comparison of Figures 1-4 reveals several distinguishing features: (1) The framework silicate data use to prepare Figure 1 are statistically identical with the predictions of the rigid bond model for a set of ordered crystals free from defects;

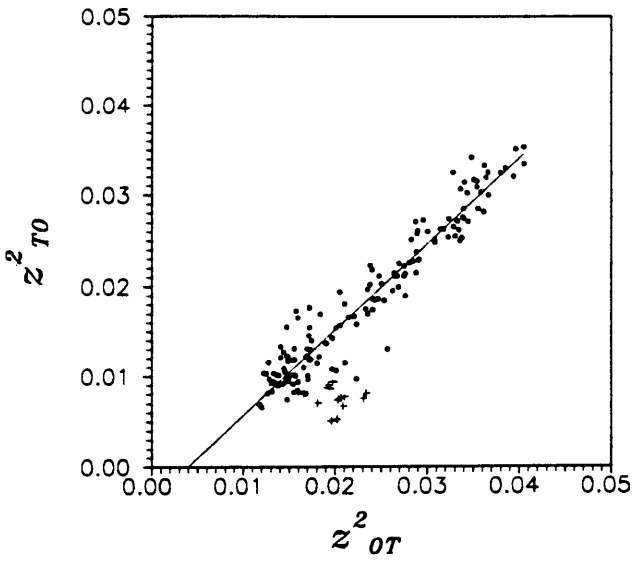

Figure 4. z^2_{TO} vs. z^2_{OT} for high albite and sanidine. Weitz data is indicated by a plus sign, +. The regression equation without the Weitz data is $z^2_{TO} = -0.0037 + 0.945 z^2_{OT}$ where $\sigma(-0.0037) = .0006\text{Å}^2$, $\sigma(0.945) = 0.023$ and the coefficient of determination is $r^2 = 0.92$.

(2) The data for the clathrasils and low tridymite scatter rather widely over much of the field of Figure 2, suggesting that these crystals contain a significant number of defects that may be ascribed to twinning and stacking faults; and (3) The data for high albite and sanidine are spread rather uniformly along a line that parallels that recorded for low albite and low microcline, but the intercept (-0.0037Å^2) of the line fit to the data, without the Eifel data, is significantly smaller than 0.0, the intercept obtained for both the framework silicates and for low albite and low microcline. The departure of the intercept from 0.0 may be ascribed to substitutional disorder. If we assume that there is complete substitutional disorder in high albite and sanidine, then, on average, 25% of the TO_4 groups would contain Al. With Bürgi's (1989) assumption that $R(SiO) = 1.607\text{Å}$ and $R(AlO) = 1.744\text{Å}$ for ordered feldspar structures (see Equation 1), the average TO bond length for the disordered structures is predicted to be 1.641Å. Substituting this value

into Bürgi's equation gives $\langle\Delta_t\rangle=\langle z^2_{OT} - z^2_{TO}\rangle = 0.0035\text{Å}^2$. This implies that $\langle z^2_{TO}\rangle = -0.0035+\langle z^2_{OT}\rangle$ predicting an intercept of -0.0035Å^2. As the slope found for the regression equation for high albite and sanidine is significantly different from 1.0, it appears that the experimental line is statistically different from that predicted by Bürgi's equation. Nevertheless, the slope of the line departs by only 1.6° from the ideal value. This small departure suggests that the experimental data conforms, to a first approximation, with the theoretical trend predicted by Bürgi's equation.

The departure of the slopes for the feldspars from the ideal 45° line may be related to an increase in the optical mode vibrations of the T and O atoms accompanying an increase in temperature at high temperatures. The feldspar data with the larger z^2-values in Figures 3 and 4, which strongly influence the slope, were recorded at temperatures as high as 1250 K. We would expect at this high temperature, that the vibrational amplitude of the lighter O atom would increase at a faster rate than the heavier T atom with increasing temperature. This would result in z^2_{OT} increasing at a faster rate that z^2_{TO}, providing a possible explanation for the departure of the slope from 45°.

The departure of the intercept of the regression line observed for high albite and sanidine from 0.0 may also be rationalized with Bürgi's equation. In his derivation of the equation, Bürgi (1989) assumed that each T atom is fixed in space regardless of whether T is Al or Si, while the coordinating oxygen atoms are located, on average, a distance of 1.744Å away when T is Al, or 1.607Å when it is Si. The substitutional disorder is argued to cause the thermal ellipsoids of the oxygen atoms to be elongated in the direction of the TO bonds, and when the disorder is complete for an Al/Si ratio of 0.25, then the amount of elongation should be fairly constant with the value of z^2_{OT} being 0.0035Å^2 larger that of z^2_{TO}

along the same bond. When the Al/Si ratio in a disordered feldspar is at its maximum value of 0.50, then Bürgi's equation yields a maximum $\langle\Delta_t\rangle$-value of 0.0047Å^2. When the $\langle\Delta\rangle$-values of a structure exceeds this value, then types of disorder other than substitutional should be considered.

Criteria for Recognizing Ordered Structures with Rigid Bonds, Structures with Substitutional Disorder and Those with Twinning and Stacking Faults

The structures of the ordered framework silicates and aluminosilicates appear to be composed of rigid TO bonds, as demonstrated by the equality of z^2_{TO} and z^2_{OT} for low albite, low microcline, quartz, cristobalite and coesite. This implies that $\langle\Delta\rangle$ should be close to zero, on average, for the bonds in these ordered structures. If we define $\langle\langle\Delta\rangle\rangle$ to be the average of all the $\langle\Delta\rangle$ values in a structure, then $\langle\langle\Delta\rangle\rangle$ should also be close to zero. Furthermore, the estimated standard deviation, esd, of $\langle\langle\Delta\rangle\rangle$, should also be small since the range of values of $\langle\Delta\rangle$ is small. A histogram of $\langle\langle\Delta\rangle\rangle$ prepared for low albite, low microcline, quartz, cristobalite and coesite (Figure 5a) shows that the $\langle\langle\Delta\rangle\rangle$-values calculated for these structures range between -0.00123 and 0.00177Å^2. The frequency distribution of esd's of the $\langle\langle\Delta\rangle\rangle$-values recorded for these structures is plotted in Figure 6a which shows a maximum esd of 0.00120Å^2. Histograms of $\langle\langle\Delta\rangle\rangle$ and its esd's prepared for the clathrasils and tridymites (Figures 5b and 6b, respectively) show a much larger range of $\langle\langle\Delta\rangle\rangle$-values than recorded for the ordered feldspars and the framework silicates coesite, quartz and low cristobalite, from -0.007 to 0.021Å^2, with esd's as large as 0.022Å^2. As mentioned earlier, regression analyses of R(SiO) as a function of several variables involving the angle within and between silicate tetrahedra, B(O), B(Si) and P for the clathrasils and the tridymite show that R(SiO) is independent of all of the variables except B(O). The fact that R(SiO) does not

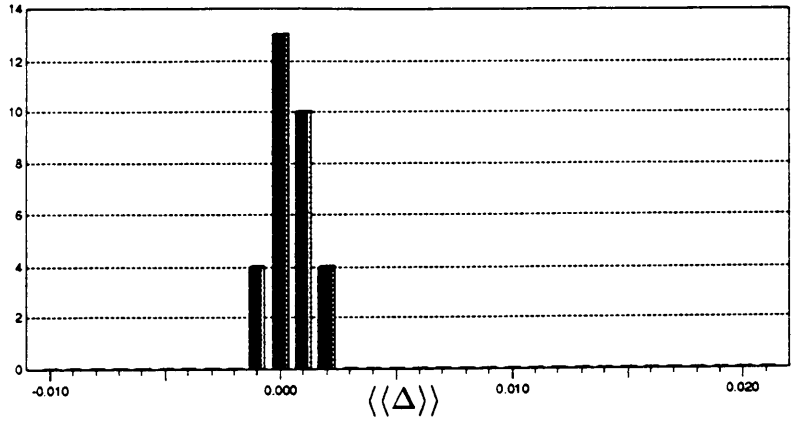

Figure 5a. Histogram of $\langle\langle\Delta\rangle\rangle$ (Å^2) for the ordered structures: low albite, low microcline, quartz, cristobalite and coesite.

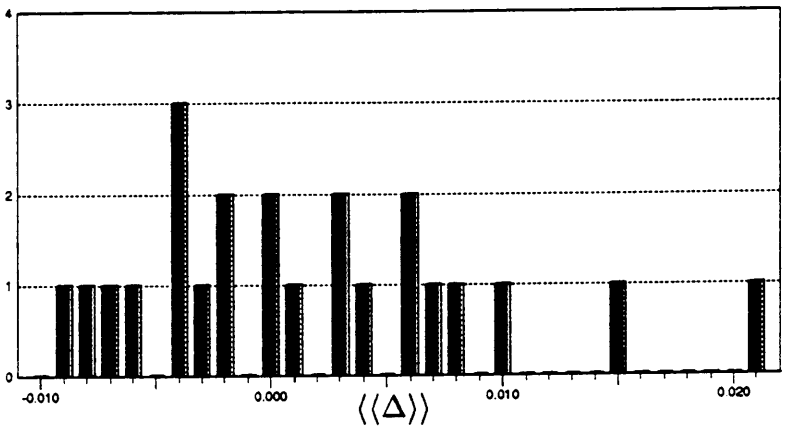

Figure 5b. Histogram of $\langle\langle\Delta\rangle\rangle$ (Å^2) for the disordered structures of tridymite and the clathrasils.

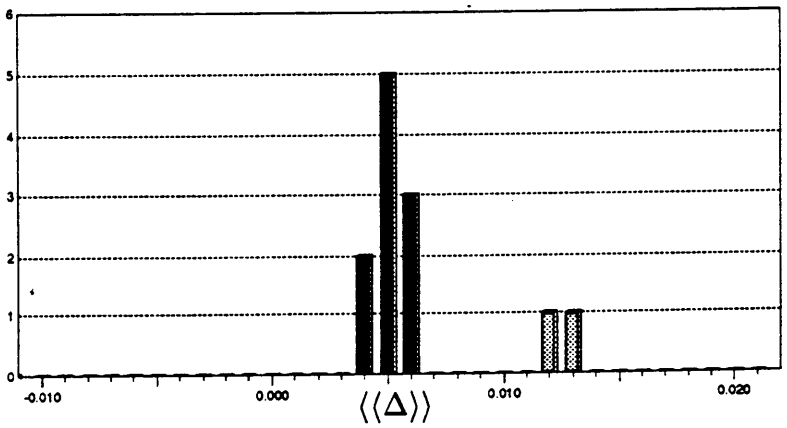

Figure 5c. Histogram of $\langle\langle\Delta\rangle\rangle$ (Å^2) for the substitutionally disordered high albite and sanidine. The Eifel sanidine is marked with cross-hatching.

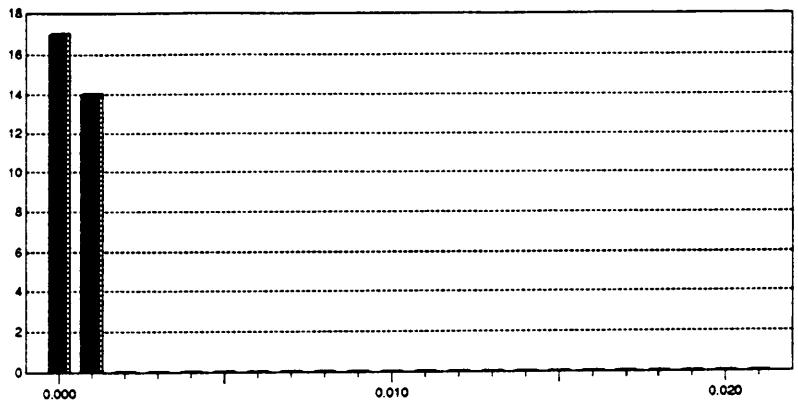

Figure 6a. Histogram of the esd's of $\langle\langle\Delta\rangle\rangle$ (Å^2) for the ordered structures: low albite, low microcline, quartz, cristobalite and coesite.

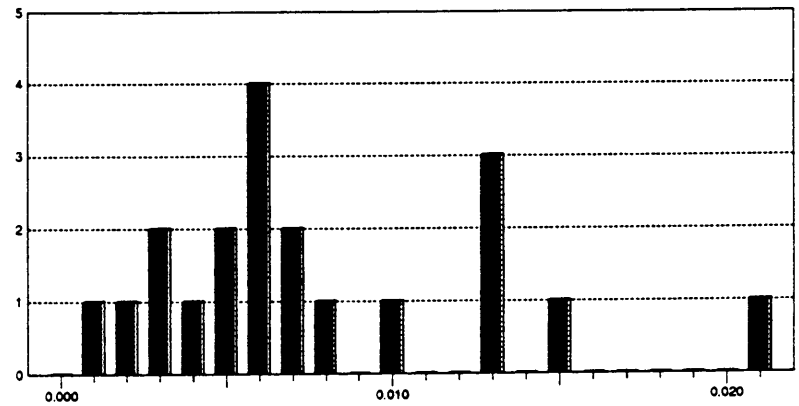

Figure 6b. Histogram of the esd's of $\langle\langle\Delta\rangle\rangle$ (Å^2) for the disordered structures of tridymite and the clathrasils.

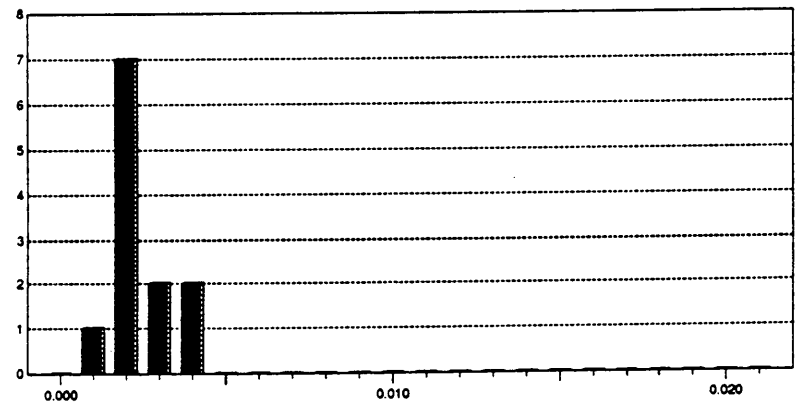

Figure 6c. Histogram of the esd's of $\langle\langle\Delta\rangle\rangle$ (Å^2) for the substitutionally disordered high albite and sanidine.

correlate with the SiOSi angle may be related to the twinning and stacking faults in these crystals.

During the past 20 years, there has been a debate in the literature as to whether R(SiO) correlates with the SiOSi angle or not (see Boisen *et al.*, 1990 for a review). Evidence in support of this correlation has been presented for the framework silicates by Gibbs *et al.*, (1972; 1977), Hill and Gibbs (1979) and Newton and Gibbs (1980). On the other hand, Baur (1971; 1977) and Baur and Ohta (1982) have concluded on the basis of regression analyses of the SiO bond length variations for a number of framework silicates including low tridymite and several silicates with p_O values of 2.0 that only 4 to 9% of the variation of SiO could be explained in terms of a linear dependence on the angle. The SiO bond length and SiOSi angle data for tridymite were obtained by Baur (1977) in a re-refinement of a set of data collected by Kato and Nukui (1976). A calculation of the $\langle\langle\Delta\rangle\rangle$ value and its esd for the low tridymite crystal refined and used by Baur (1977) and by Baur and Ohta (1982) in their studies yields values of 0.00077Å^2 and 0.00345Å^2, respectively. A plot of $z^2_{Si,O}$ vs. $z^2_{O,Si}$ calculated for the SiO bonds in the tridymite crystal is given in Figure 7. This data shows a wide range of values like that for the clathrasils and tridymites which was ascribed to the presence of twinning and stacking faults. We note that Kato and Nukui (1976) were careful to observe in their structure analysis of the mineral that it was twinned about the [301]. Thus the data used by Baur (1977) in his re-refinement of the structure was obtained from a twinned crystal, possibly containing stacking faults, making it unsuitable for establishing whether or not a correlation exists between R(SiO) and the SiOSi angle. In view of these results, it is understandable why Baur (1977) found that only 4% of the variation of R(SiO) can be explained in terms of a linear dependence on $-\sec$(SiOSi), particularly when it is recalled that 48

of the 60 bond lengths in the data used in his regression analysis were recorded from a tridymite crystal that is twinned and possesses static disorder. It is clear from this observation that Baur's conclusions about that the correlation between R(SiO) and – sec(SiOSi) are not well-founded and therefore should be discounted.

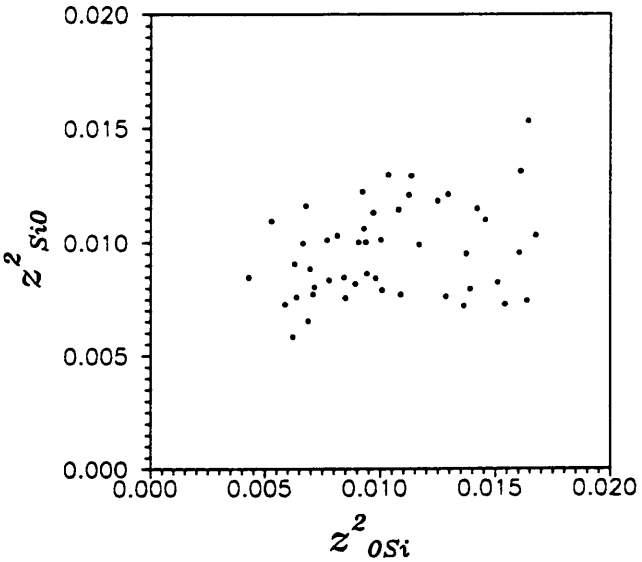

Figure 7. A scatter plot of z^2_{SiO} versus z^2_{OSi} for the tridymite data of Baur (1977) showing a lack of evidence for rigid bonding and therefore suggesting disorder, perhaps due to twinning about [301].

Histograms of $\langle\langle\Delta\rangle\rangle$ and its esd's prepared for the disordered feldspars sanidine and high albite are presented in Figures 5c and 6c, respectively. All of these data, with the exception of the Eifel sanidine data, fall within the range of $\langle\langle\Delta\rangle\rangle$-values of 0.0037 to 0.0050Å^2, the range expected for disordered feldspar with Al/Si ratios between 0.25 and 0.50. The $\langle\langle\Delta\rangle\rangle$-values for the Eifel sanidine (0.012-0.013Å^2) fall outside this range. In fact, the values are similar to those exhibited by the clathrasils and the tridymites. Recall that the data for the Eifel sanidine falls off the general trend of defined in Figure 4. In view of the large $\langle\langle\Delta\rangle\rangle$-values recorded for this feldspar, the evidence suggest that it may contain submicroscopic-twinning

and stacking faults as indicated for the clathrasils and the tridymites. This would provide an explanation for why the Eifel data fall off the linear trend in Figure 4.

Based on the histograms for the ordered feldspars and silica polymorphs (Figures 5a and 6a), a rigid bond criteria for TO bonds in framework structures is suggested that may be used to define the order of a crystal. If the *TO* bonds in an ordered structure are rigid, then the following criteria should be satisfied: (1) $-0.00125 Å^2 \leq \langle\langle\Delta\rangle\rangle \leq 0.002$ Å^2 and (2) the esd's of $\langle\langle\Delta\rangle\rangle$ be less than 0.00125 Å^2. In an application of these two criteria, we calculated the $\langle\langle\Delta\rangle\rangle$-values and their esd's for 138 framework silicate and aluminosilicate structures. Those that satisfy the two criteria are listed in Table 1 and those that fail are listed in Table 2.

A discussion of the data of Tables 1 and 2 is in order. Five of the quartz refinements examined satisfy the rigid-bond criteria while four do not. The quartz data published by Lager *et al.*, (1982) was determined from a refinement of powder data rather than from single crystal data. As a single crystal data set is usually more precise and larger in size than a powder data set, the failure of the Lager data set to satisfy both criteria is not unexpected. The Smith and Alexander (1963) data set appears to have been refined with wrong symmetry constraints imposed on the displacement parameters of the atoms (Zachariasen and Plettinger, 1965), thus explaining the failure of the criteria for this quartz refinement. The quartz data presented by Zachariasen and Plettinger, (1965) were obtained in refinements where two different extinction correction models were tested. The quartz structure refined with their type II model passed the criteria whereas that refined with the type I failed, suggesting that the type II model may be the more appropriate extinction model. The high quartz structure refinements passed both criteria even though the data were recorded at high temperature (862 K). In all the cases examined for quartz, failure to satisfy the criteria seems to depend on

the refinement procedures and how the data were recorded and to be independent of the crystals themselves. This is surprising because of the ubiquity of twinning in quartz (Frondel, 1962).

All of the refinements for low cristobalite undertaken by Peacor (1973) pass the criteria with the exception of the one undertaken at 502 K. The failure of this refinement is, however, marginal. All three of the low cristobalite refinements completed by Pluth *et al.*, (1985) fail. From their refined parameters, the Si atom was always found to vibrate with a larger amplitude along the SiO bond than the O atom, unlike all the other structures in Table 1, where O has the larger amplitude. We offer no explanation for this result. Without exception, all the coesite structures satisfy the criteria, as we expected, inasmuch as these data were used to established the criteria. On the other hand, all the tridymite and clathrate structures examined in our study fail the criteria.

All the low albite refinements examined satisfy the criteria. Like the data for coesite, they also were used to establish the criteria and so this was not an unexpected result. In an examination of the Winter *et al.*, (1977) study for low albite, a regular increase in $\langle\langle\Delta\rangle\rangle$ and its esd is observed to occur with increasing temperature. As indicated earlier, this supports the suggestion that the TO bonds in this material weaken with increasing temperature. The "ordered orthoclase" crystal refined by Prince *et al.*, (1973) also fails the criteria. A study of the mean TO bond lengths of this mineral indicates that the T(2) tetrahedra are Si rich whereas the T(1) tetrahedra contains a disordered occupancy of one Al and one Si, on average. An examination of the $\langle\Delta\rangle$-values and their esd's for these two tetrahedra yield values that agree with these results (T(2):$\langle\Delta\rangle$= -0.00023Å^2, esd = 0.00138Å^2; T(1):$\langle\Delta\rangle$= 0.00466Å^2, esd = 0.00590Å^2). The $\langle\Delta\rangle$-value calculated for the T(1) tetrahedron that contains 0.5Al and 0.5Si , on average, agrees with

a value of 0.0047Å^2 calculated with the Bürgi equation for a disordered array of Al and Si over the T(1) tetrahedron. The $\langle\Delta\rangle$-value for the T(2) tetrahedron indicates the tetrahedron is ordered and only contains Si as determined from its mean TO bond lengths.

None of anorthite crystals that we examined passes the criteria. Angel (1988) refined the Val Pasmeda anorthite in both $I\bar{1}$ and $P\bar{1}$ settings, and we found that the $P\bar{1}$ refinement comes the closest to satisfying the criteria, supporting suggestions that the $P\bar{1}$ setting is the more appropriate setting for anorthite. Angel's results and those recorded by Czank (1973), Kalus (1978) and Wenk and Kroll (1984) for anorthite suggest that these crystals may exhibit a small amount of substitutional disorder despite an Al/Si ratio of 1.0.

Seven of the eighteen structural refinements completed for cordierite and listed in Table 2 fail the criteria. This failure does not seem to be related to the wide range of Fe-Mg substitution exhibited by these materials. We are unable to offer a satisfactory explanation for these failures.

Of the 32 refinements of zeolites examined in our study 7 (edingtonite (2X), mesolite, natrolite, scolecite, thomsonite and yugawaralite) satisfy the criteria while the remaining ones fail. All 7 of the zeolites that satisfied the criteria are considered to be ordered, within the experimental error, in terms of their mean TO bond lengths. Of the 25 zeolites that failed, 22 are considered to exhibit substitutional disorder. A calculation of the TO bond lengths for one of these zeolites, analcime, using data published by Pechar (1988) yields the following mean TO bond lengths and predicted occupancies: $\langle$Si1O$\rangle$ = 1.614, 0.06 Al; $\langle$Si2O$\rangle$ = 1.621, 0.11 Al; $\langle$Si3O$\rangle$ = 1.621, 0.11 Al; $\langle$Si4O$\rangle$ = 1.614, 0.06 Al; $\langle$Al1O$\rangle$ = 1.740, 0.89 Al and $\langle$Al2O$\rangle$ = 1.740, 0.89 Al. These results indicate a moderate degree of disorder with a long range order parameter of s = 0.78. However, a $\langle\langle\Delta\rangle\rangle$-

value of 0.0046Å^2 calculated for this zeolite indicates a completely disordered structure. This discrepancy is not understood. A $\langle\langle\Delta\rangle\rangle$-value of 0.00065Å^2 and an esd of 0.00197Å^2 calculated for the zeolite gismondine suggests a small amount of disorder, in agreement with the Artioli *et al.*(1986) statement that the mean TO distances in the zeolite "are consistent with an essentially ordered distribution of Si and Al and the possibility of a minor substitution of excess Si in the Al(1) site". An examination of the mean TO bond lengths in goosecreekite (Rouse and Peacor, 1986) indicates almost complete Si/Al ordering. However, a large $\langle\langle\Delta\rangle\rangle$-value of 0.00715Å^2 calculated for this zeolite indicates the presence of structural disorder possibly in the form of stacking faults or twinning. For the edingtonites refined in a study, Mazzi *et al.*, (1984) concluded them to be completely disordered. The $\langle\langle\Delta\rangle\rangle$ and the esd's calculated for these zeolites conform with this result. The Cd-X zeolite refined by Calligaris *et al.*, (1986) shows, after dehydration, a substantial increase in Δ-values with the $\langle\langle\Delta\rangle\rangle$-values increase from 0.00458Å^2 to 0.01707Å^2. This suggests that dehydration may induce some form of disorder.

The Preferred Orientation of the Displacement Ellipsoids of the O Atoms in Framework Structures

The force required to distort a SiO bond within the silicate tetrahedra of a framework structure is much larger than that required to distort a SiOSi angle between the tetrahedra. Consequently, the vibrational frequencies associated with a SiO stretching mode ($\sim$1100 cm^{-1}) are significantly larger than those associated with SiOSi bending mode. ($\sim$200-400 cm^{-1}) (Lasaga and Gibbs, 1988). From these results, it can be argued that the amplitudes of vibration in those directions that require little or no SiO bond stretching should be larger than those in other direction that require bond stretching. For example, vibrations of the bridging

O atom in the direction perpendicular to a SiOSi plane would require little or no SiO bond stretching and so this would correspond with the direction of its largest amplitude. Thus, the MSDA for the O atom should be the largest in this direction. On the other hand, vibrations of the atom parallel to the SiSi direction would entail much more SiO bond stretching and so this would correspond with the direction of its smallest vibrational amplitude. Accordingly, the MSDA for the O atom should be smallest in this direction. Also, we may expect that the extent to which the ellipsoids show such a preferred orientation would depend on the size of the SiOSi angle. For example, those O atoms involved in narrow angles should have the major axes of their displacement ellipsoids tightly constrained at about 90° to the SiOSi plane. On the other hand, as the angle widens, this constraint should be relaxed and a wider range of orientations may be expected. As we shall see, the observed orientations of the displacement ellipsoids for the O atoms in many of the structures listed in Table 1 conform with these arguments.

Figures 1 and 3 show that the displacement ellipsoids of the O atoms in the ordered framework silicates and aluminosilicates are constrained so that the MSDA's of each O comprising a TO bond tends to equal that of the T atom, in the direction of the TO bond. In a study of the ellipsoids of the O atoms in orthopyroxene, Burnham *et al.* (1971) observed that the major axis of the ellipsoid for the bridging O atom in that structure is constrained to be perpendicular to the SiOSi plane. A similar observation was reported for the orientation of the ellipsoids of the O atoms in β-eucryptite by Tscherry *et al.* (1972), but he questioned whether this was related to thermal motion. He based this argument on the lack of any such preferred orientation of the ellipsoids of the O atoms in quartz. On the other hand, Schulz (1972) observed that the displacement ellipsoids of the O atoms in the framework aluminosilicates tend to be oriented with their

major axes perpendicular to the TOT plane, their minor axes parallel to the TT direction and their intermediate axes lying in the TOT plane perpendicular to the TT direction.

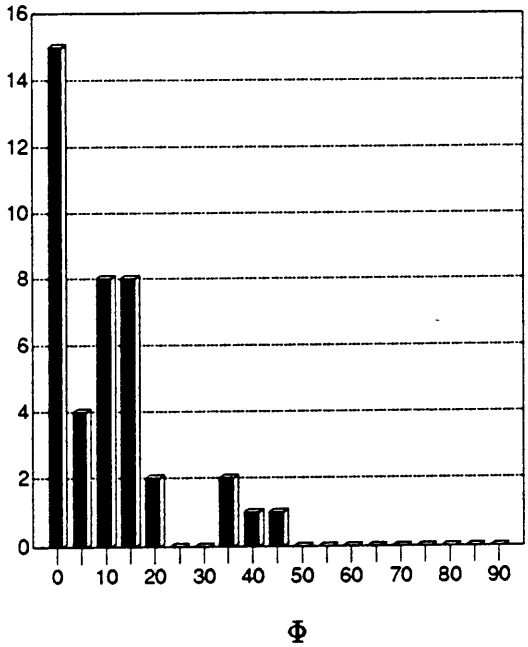

Figure 8. A histogram of the angle Φ for the quartz, cristobalite and coesite structures which satisfy our criteria.

Consider a plane bisecting a TOT angle and intersecting the displacement ellipsoid of a bridging O atom. The intersection of this plane with the ellipsoid defines an ellipse with major and minor axes. (See Appendix 1 for a description of the method used to find the magnitudes and directions of the axes.) When the TOT angle is not 180°, we define Φ to be the acute angle between this major axis and the normal to the TOT plane. To explore the extent to which the O atoms in the ordered framework silicates are constrained as described by Schulz (1972), we prepared the frequency diagram displayed in Figure 8. A Φ-value of 0° means that the major axis of the ellipse is perpendicular to the SiOSi plane whereas a value of 90° means that the minor axis is perpendicular to the plane. An examination of this figure shows that 90% of the O atoms have the major axes of their cross

sectional ellipsoids oriented within 20°of the perpendicular to the SiOSi plane.

The Φ angles were also calculated for the aluminosilicate data in Table 1 to learn how their angles are distributed (Figure 9) relative to those of the framework silicates. Despite the presence of nontetrahedral cations in the aluminosilicates, which could affect the orientation of the displacement ellipsoid, 80% of the Φ angles fall between 0 and 20°. This compares rather well with that observed for the framework silicates and suggests that the nontetrahedral cations play little or no role in controlling the preferred orientations of the displacement ellipsoids for the O atoms.

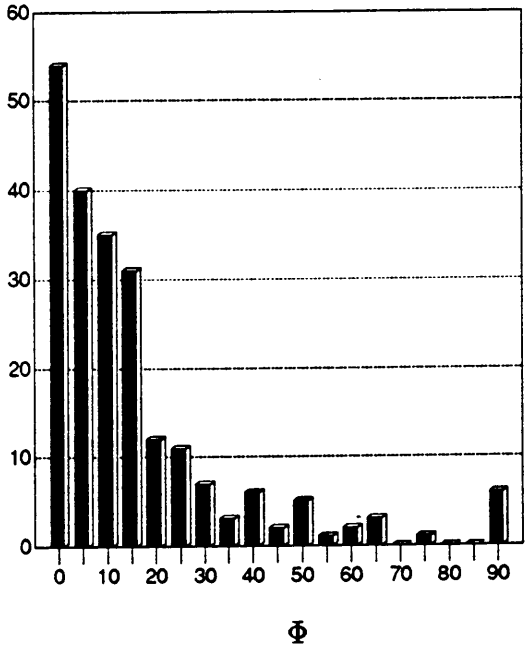

Figure 9. A histogram of the angle Φ for the framework aluminosilicates which satisfy our criteria.

If the orientation of these displacement ellipsoids is related to the magnitude of the TOT angle, as argued above, then a plot of Φ vs. the TOT angle should show an increasing range of values for Φ as the angle widens to 180°. Such a plot is present in Figure 10 where we see a progressive increase in the range of Φ values as the TOT angle widens. Out of curiosity, we prepare a similar plot (Figure

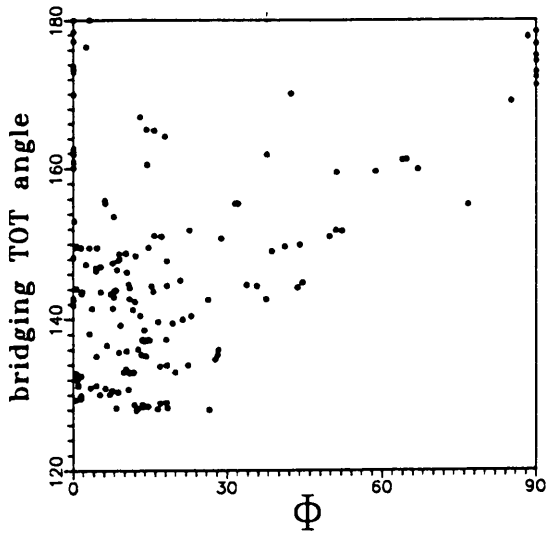

Figure 10. A scatter plot of Φ versus the bridging TOT angle for the silica polymorphs and aluminosilicates that satisfy the rigid-bond criteria.

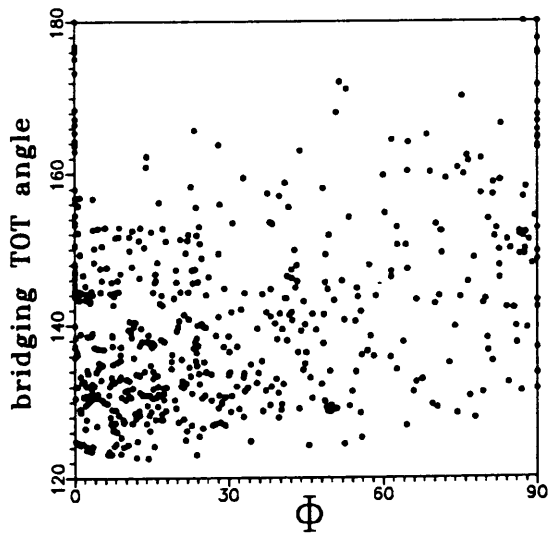

Figure 11. A scatter plot of Φ versus the bridging TOT angle for the aluminosilicates and silica polymorphs which failed the rigid-bond criteria.

11) for all the structures listed in Table 2. For these structures, we see that the displacement ellipsoid of the O atoms has no preferred orientation relative to the

TOT angle.

Conclusions

At the conclusion of an International Union of Crystallographers Conference on accurate measurements of X-ray diffraction data and structural amplitudes for well-ordered crystals, Zachariasen (1969) made the important observation that the positional parameters obtained from X-ray measurements, made up till that time, are reasonably good and make sense while the ADP's "are all nonsense and must all be done again in a sensible way". The following year, this observation was borne out by a study of 17 different sets of diffraction data recorded by different workers for D(+)-tartaric acid (Hamilton and Abrahams, 1970). Independent least-squares refinements of these data sets yielded 17 separate sets of positional parameters. A comparison of these parameters shows reasonable agreement, but an examination of associated sets of ADP's shows poor agreement. This may explain why the ADP's obtained in a structural analysis are rarely used to understand the crystal other than perhaps in the generation of an ORTEP drawing of its crystal structure (Dunitz, 1985).

The data recorded for coesite at room temperature and 1 atm. by Gibbs *et al.* (1977), Levien and Prewitt (1981), Kirfel and Will (1984), Smyth *et al.* (1986) and Geisinger *et al.* (1987) provide 6 independently measured data sets that may be studied to learn whether such poor agreement exists today among data sets, despite improvements that have made during the last 10 years in measuring and reducing diffraction data to structural amplitudes. An examination of the bond lengths and angles calculated by these workers show that they are statistically identical with one another, on average. Similarly, the magnitudes of the principal axes of the displacement ellipsoids and their orientation angles (Table 3)

calculated from the 6 independently determined sets of ADP's also show close agreement. These results demonstrate that sensible sets of positional and displacement parameters can be obtained in an X-ray study of ordered crystals like those listed in Table 1. Our study of the ADP's obtained for these crystals also shows that important information can be obtained about crystal perfection and the rigid-body motion.

Table 1. Silica Polymorphs and Aluminosilicate Frameworks Which Satisfy Our Rigid-Bond Criteria

Mineral	Reference	$\langle\langle\Delta\rangle\rangle$	esd.
quartz	Young and Post, (1962)	−0.00073	0.00023
quartz	Zachariasen and Plettinger, (1965), type II	0.00187	0.00022
quartz	LePage and Donnay, (1976)	0.00056	0.00003
quartz	Levien et al., (1980)	0.00082	0.00021
quartz	Wright and Lehmann, (1981), at 25°C	−0.00014	0.00050
high quartz	Wright and Lehmann, (1981), natural at 590°C	−0.00022	0.00004
high quartz	Wright and Lehmann, (1981), synthetic at 590°C	−0.00051	0.00005
cristobalite	Peacor, (1973), at 28°C	0.00001	0.00063
cristobalite	Peacor, (1973), at 65°C	−0.00123	0.00002
cristobalite	Peacor, (1973), at 103°C	0.00076	0.00128
cristobalite	Peacor, (1973), at 142°C	−0.00063	0.00081
cristobalite	Peacor, (1973), at 179°C	0.00170	0.00117
cristobalite	Peacor, (1973), at 210°C	0.00105	0.00090
coesite	Gibbs et al., (1977)	0.00007	0.00056
coesite	Levien and Prewitt, (1981)	0.00045	0.00032
coesite	Kirfel and Will, (1984)	0.00003	0.00018
coesite	Smyth et al., (1987), at 15K	0.00026	0.00041
coesite	Smyth et al., (1987), at 292K	0.00054	0.00016
coesite	Geisinger et al., (1987), IAM refinement	0.00004	0.00010
coesite	Geisinger et al., (1987), IAM+ refinement	−0.00046	0.00024
low albite	Winter et al., (1977), at 500°C	0.00130	0.00061
low albite	Winter et al., (1977), at 750°C	0.00135	0.00062
low albite	Winter et al., (1977), at 970°C	0.00156	0.00098
low albite	Harlow and Brown, (1980), neutron	0.00035	0.00035
low albite	Harlow and Brown, (1980), X-ray	0.00177	0.00090
low albite	Smith et al., (1986), at 13K	0.00035	0.00018
low albite	Armbruster et al., (1990)	0.00028	0.00033
microcline	Strob, (1981)	−0.00005	0.00027
microcline	Blasi et al., (1984), sample 7813A	0.00115	0.00120
microcline	Blasi et al., (1984), sample 7813B	0.00060	0.00116
microcline	Blasi et al., (1987)	0.00085	0.00078
slawsonite	Griffen et al., (1977)	0.00125	0.00096
low cordierite	Cohen et al., (1977), X-ray	0.00136	0.00086
low cordierite	Cohen et al., (1977), neutron	0.00058	0.00093
low cordierite	Hochella et al., (1979), at 375°C, White Well	0.00001	0.00133
low cordierite	Wallace and Wenk, (1980), sample Sci 624	0.00108	0.00073
low cordierite	Wallace and Wenk, (1980), sample Sci 1018	0.00191	0.00057
low cordierite	Armbruster, (1986a), from Ferry	0.00073	0.00066
low cordierite	Armbruster, (1986a), from Haddam	0.00059	0.00057
low cordierite	Armbruster, (1986a), from Sponda	0.00048	0.00058
low cordierite	Armbruster, (1986a), from Kemiö	0.00069	0.00118
low cordierite	Armbruster, (1986b), at 100K	0.00062	0.00062
low cordierite	Armbruster, (1986b), at 500K	0.00027	0.00064
bikitaite	Bissert and Liebau, (1986)	0.00061	0.00082
edingtonite	Galli, (1976)	0.00097	0.00117
edingtonite	Kvick and Smith, (1983)	0.00066	0.00063
mesolite	Artioli et al., (1986)	0.00057	0.00061
natrolite	Artioli et al., (1984)	0.00040	0.00031
scolecite	Kvick et al., (1985)	0.00040	0.00026
thomsonite	Pluth et al., (1985)	0.00060	0.00048
yugawaralite	Kvick et al., (1986)	0.00084	0.00059

Table 2. Silica Polymorphs and Aluminosilicate Frameworks
Which Do Not Satisfy Our Rigid-Bond Criteria

Mineral	Reference	$\langle\langle\Delta\rangle\rangle$	esd.
quartz	Lager et al., (1982), at 13K	0.00264	0.00144
quartz	Lager et al., (1982), at 78K	0.00284	0.00165
quartz	Smith and Alexander, (1963)	0.00266	0.00086
quartz	Zachariasen and Plettinger, (1965), type I	0.00211	0.00013
cristobalite	Peacor, (1973), at 230°C	−0.00092	0.00176
cristobalite	Pluth et al., (1985), at 10K	−0.00146	0.00040
cristobalite	Pluth et al., (1985), at 293K	−0.00555	0.00174
cristobalite	Pluth et al., (1985), at 473K	−0.00777	0.00299
tridymite	Dollase, (1967)	0.00522	0.00773
tridymite	Baur, (1977)	0.00077	0.00345
tridymite	Kihara, (1977)	0.00424	0.02162
tridymite	Kihara, (1978)	0.00175	0.00718
tridymite	Kihara et al., (1986a), at 443K	0.01423	0.01261
tridymite	Kihara et al., (1986a), at 493K	0.00408	0.01008
tridymite	Kihara et al., (1986a), at 573K	0.00574	0.00618
tridymite	Kihara et al., (1986a), at 653K	0.00834	0.01277
tridymite	Kihara et al., (1986a), at 693K, $C222_1$	−0.00051	0.00623
tridymite	Kihara et al., (1986a), at 693K, $P6_3/mmc$	−0.00485	0.00640
tridymite	Kihara et al., (1986a), at 733K, $P6_3/mmc$	−0.00310	0.00678
tridymite	Kihara et al., (1986b), at 493K	−0.00652	0.00427
tridymite	Kihara et al., (1986b), at 693K	−0.00255	0.00534
tridymite	Kihara et al., (1986b), at 733K	−0.00088	0.00582
melanophlogite	Gies, (1983)	−0.00204	0.00113
dodecasil 3C	Gies, (1984)	−0.00265	0.00549
dodecasil 1H	Gerke and Gies, (1984)	0.00101	0.01453
dodecasil 3R	Gies, (1986)	0.02163	0.01340
high albite	Keefer and Brown, (1978)	0.00415	0.00331
high albite	Winter et al., (1979), at 25°C	0.00388	0.00141
high albite	Winter et al., (1979), at 500°C	0.00500	0.00155
high albite	Winter et al., (1979), at 750°C	0.00537	0.00211
high albite	Winter et al., (1979), at 980°C	0.00508	0.00191
intermediate albite	Phillips et al., (1989)	0.00392	0.00152
microcline	Blasi et al., (1981)	0.00461	0.00369
adularia	Phillips and Ribbe, (1973)	0.00600	0.00357
sanidine	Keefer and Brown, (1978)	0.00491	0.00160
sanidine	Phillips and Ribbe, (1973)	0.00643	0.00152
sanidine	Scambos et al., (1987)	0.00560	0.00174
sanidine	Weitz, (1972), Eifel, unheated	0.01282	0.00219
sanidine	Weitz, (1972), Eifel, heated	0.01218	0.00255
orthoclase	Prince et al., (1973)	0.00304	0.00530
celsian	Griffen and Ribbe, (1976)	0.00472	0.00515
$Cs[AlSi_5O_{12}]$	Araki, (1980)	0.00203	0.00249
$RbAlSiO_4$	Klaska and Jarchow, (1975)	0.00333	0.00111

Table 2. (continued) Silica Polymorphs and Aluminosilicate Frameworks Which Do Not Satisfy Our Rigid-Bond Criteria

Mineral	Reference	$\langle\langle\Delta\rangle\rangle$	esd.
plagioclase	Tagai et al., (1980), An66	0.00327	0.01002
anorthite	Czank, (1973), $P\bar{1}$ at 20°C	0.00338	0.00298
anorthite	Czank, (1973), $P\bar{1}$ at 240°C	0.00175	0.00381
anorthite	Kalus, (1978), $P\bar{1}$	0.00058	0.00204
anorthite	Wenk and Kroll, (1984), An94, $P\bar{1}$	0.00242	0.00141
anorthite	Angel, (1988), sample 115082a $I\bar{1}$	0.00111	0.00227
anorthite	Angel, (1988), from Monte Somma, $I\bar{1}$	0.00047	0.00216
anorthite	Angel, (1988), from Val Pasmeda, $I\bar{1}$	0.00130	0.00365
anorthite	Angel, (1988), from Val Pasmeda, $P\bar{1}$	0.00018	0.00208
Sr feldspar	Chiari et al., (1975)	0.00205	0.00408
Sr feldspar	Grundy and Ito, (1974)	0.00311	0.00302
low cordierite	Hochella et al., (1979), at 24°C, Dolni Bory	0.00150	0.00203
low cordierite	Hochella et al., (1979), at 375°C, Dolni Bory	−0.00009	0.00301
low cordierite	Hochella et al., (1979), at 775°C, White Well	−0.00012	0.00358
low cordierite	Wallace and Wenk, (1980), sample Brg 50	0.00343	0.00140
low cordierite	Wallace and Wenk, (1980), sample Sci 552	0.00239	0.00080
low cordierite	Wallace and Wenk, (1980), sample Sci 1542	0.00276	0.00069
low cordierite	Wallace and Wenk, (1980), sample Sci 1104	0.00277	0.00102
analcime	Pechar, (1988)	0.00464	0.00274
bicchulite	Sahl, (1980)	0.00506	—
brewsterite	Schlenker et al., (1977)	0.00462	0.00204
chabazite	Mortier et al., (1979)	0.00836	0.00169
clinoptilolite	Koyama and Takéuchi, (1977), from Agoura	0.00430	0.00249
clinoptilolite	Koyama and Takéuchi, (1977), from Kuruma	0.00200	0.00362
edingtonite	Mazzi et al., (1984), Ice River	0.00444	0.00059
edingtonite	Mazzi et al., (1984), Old Kilpatrick	0.00430	0.00075
ferrierite	Vaughan, (1966)	0.01042	0.01388
ferrierite	Gramlich-Meier et al., (1984)	0.00382	0.00895
ferrierite	Gramlich-Meier et al., (1985)	0.00563	0.00766
ferrierite	Alberti and Sabelli, (1987)	0.00380	0.00655
gismondine	Artioli et al., (1986)	0.00065	0.00197
goosecreekite	Rouse and Peacor, (1986)	0.00715	0.00541
osumilite	Armbruster and Oberhänsli, (1988)	0.00318	0.00340
mordenite	Alberti et al., (1986)	0.00371	0.00483
offretite	Mortier et al., (1976a)	0.00603	0.00541
offretite	Mortier et al., (1976b)	0.00697	0.00466
scolecite	Joswig et al., (1984)	0.00110	0.00194
stellerite	Galli and Alberti, (1975)	0.01714	0.01552
stellerite	Miller and Taylor, (1985)	0.00820	0.00782
Cd-X zeolite	Calligaris et al., (1986), hydrated	0.00458	0.00706
Cd-X zeolite	Calligaris et al., (1986), dehydrated	0.01707	0.01128
Na-X zeolite	Calestani et al., (1987)	0.00938	0.00860
Ca-A zeolite	Thöni, (1975)	−0.00270	0.00736
Tl-A zeolite	Thöni, (1975)	−0.00358	0.00602

Table 3. A Comparison of the Displacement Ellipsoids of Si and O in Coesite

		AXIS 1				AXIS 2				AXIS 3			
Ref	B_{iso}	rms	a	b	c	rms	a	b	c	rms	a	b	c
Si1													
1	0.477	0.066	66	30	87	0.079	36	79	27	0.087	65	63	63
2	0.424	0.065	66	36	81	0.073	50	87	11	0.081	51	54	83
3	0.377	0.056	61	31	84	0.069	36	67	38	0.080	72	70	53
4	0.399	0.063	66	33	84	0.071	58	84	6	0.078	42	57	89
5	0.373	0.060	67	34	82	0.069	51	86	10	0.076	48	56	85
6	0.364	0.044	78	17	85	0.079	13	99	52	0.076	85	66	38
Si2													
1	0.487	0.072	62	54	36	0.079	55	40	58	0.084	48	75	74
2	0.429	0.065	64	85	7	0.074	63	28	83	0.081	39	63	89
3	0.372	0.062	40	89	19	0.065	83	13	85	0.077	50	77	72
4	0.398	0.064	68	77	15	0.071	61	29	75	0.077	40	65	89
5	0.371	0.061	66	79	13	0.069	62	28	77	0.075	38	65	90
6	0.366	0.069	69	88	11	0.055	84	7	89	0.079	22	84	81
O1													
1	0.767	0.069	56	39	88	0.106	76	62	53	0.114	38	66	37
2	0.703	0.063	72	23	88	0.102	55	68	71	0.111	41	84	20
3	0.681	0.061	68	27	88	0.103	35	63	84	0.107	64	85	6
4	0.679	0.064	63	32	89	0.098	79	66	47	0.110	29	70	43
5	0.641	0.053	61	34	89	0.101	73	64	54	0.106	34	71	35
6	0.643	0.044	72	21	90	0.107	77	84	29	0.104	23	70	72
O2													
1	0.719	0.094	90	0	90	0.078	45	90	15	0.112	45	90	75
2	0.701	0.097	90	0	90	0.068	58	90	1	0.113	32	90	89
3	0.628	0.091	90	0	90	0.066	51	90	9	0.106	39	90	81
4	0.611	0.091	90	0	90	0.063	58	90	2	0.104	32	90	88
5	0.577	0.091	90	0	90	0.055	56	90	4	0.103	34	90	86
6	0.586	0.084	90	0	90	0.065	59	90	5	0.105	31	90	89
O3													
1	0.804	0.071	21	75	47	0.105	88	42	54	0.120	69	52	65
2	0.788	0.076	23	80	40	0.103	79	56	54	0.117	70	36	76
3	0.736	0.067	22	79	42	0.102	86	41	58	0.115	69	51	66
4	0.743	0.070	23	76	43	0.098	80	63	48	0.118	70	30	82
5	0.710	0.064	21	79	42	0.098	80	60	51	0.115	71	33	77
6	0.720	0.074	25	72	45	0.093	95	35	57	0.114	65	61	63
O4													
1	0.881	0.078	76	72	47	0.107	64	35	57	0.126	29	61	61
2	0.854	0.073	80	72	43	0.108	67	31	60	0.125	25	65	61
3	0.805	0.075	77	67	48	0.104	67	36	55	0.119	26	64	61
4	0.802	0.066	77	73	46	0.104	67	32	60	0.124	27	63	60
5	0.763	0.060	77	74	46	0.103	65	34	59	0.121	29	62	60
6	0.782	0.066	76	63	51	0.099	82	31	60	0.125	16	76	54
O5													
1	0.774	0.071	85	6	85	0.101	7	85	65	0.119	85	86	26
2	0.756	0.077	84	7	84	0.098	8	85	66	0.115	84	85	25
3	0.719	0.067	82	8	84	0.094	8	82	63	0.118	87	87	28
4	0.717	0.070	77	13	81	0.097	14	78	67	0.113	84	86	25
5	0.684	0.067	78	12	97	0.093	13	78	66	0.113	85	87	25
6	0.700	0.051	85	5	93	0.099	8	94	66	0.119	95	88	25

References: (1) Gibbs etal. (1977), (2) Levien and Prewitt (1981), (3) Smyth etal. (1987), (4) Geisinger etal. (1987) IAM refinement, (5) Geisinger etal. (1987) IAM+ refinement, (6) Kirfel and Will (1984)

APPENDIX

A Review of Harmonic Temperature Factors

Introduction

It is well established that an atom in a crystal vibrates about its equilibrium position. This vibration can be attributed to thermal and zero-point energy. Even in a rigid framework structure like coesite the magnitudes of the vibrations can be appreciable. For instance, the O(1) atom is found to have an average amplitude of vibration in the plane perpendicular to the Si(1)Si(1) vector of 0.19Å at 15K and 0.3Å at 292K (Smyth, 1987). Therefore, in a crystal structure refinement, it is imperative not only to find the mean position of an atom, but also to describe the region in space where there is a high likelihood of finding it. This can be done mathematically with a probability distribution function (p.d.f.). If we assume harmonic restoring forces between the atoms, or in other words, that the forces between the atoms obey Hooke's Law, then it can be shown that the p.d.f. must be represented by a Gaussian function (Willis and Pryor, 1975 p92). Other uncertainties are also be represented by this p.d.f., as for instance, substitutional and lattice defects or positional disorder.

The Relationship Between Temperature Factor and Probability Distribution Function

During a typical crystal structure refinement, the recorded intensity of a X-ray beam, diffracted from a large number of reciprocal-lattice vectors, $\mathbf{s}$, ($[\mathbf{s}]^t_{D^*} = [h \quad k \quad l]$), (for a review of the notation, see Boisen and Gibbs, 1985) is converted to a set of structure amplitudes, $|F(\mathbf{s})|$. The set of observed amplitudes is compared to a set of structure amplitudes calculated with the equation

$$F(\mathbf{s}) = \sum_{j=1}^{n} f_j^h(\mathbf{s}) e^{2\pi i \mathbf{r}_j \cdot \mathbf{s}} \qquad (1)$$

where n is the number of atoms in the unit cell, $f_j^h(\mathbf{s})$ is the hot atomic scattering factor, and $\mathbf{r}_j$ represents the positional vector of the jth atom in direct space. The difference between the measured and calculated amplitudes is then minimized by varying $\mathbf{r}_j$ and $f_j^h(\mathbf{s})$. The value of $\mathbf{r}_j$ obtained in this minimization procedure represents the final atomic coordinates for atom j.

The hot atomic scattering factor, $f^h(\mathbf{s})$, represents the effect that the various electron distributions, from the various atoms in the structure, have on X-ray scattering. There are two terms implicit to this factor. The first is an electron distribution term which, essentially, is due to core electrons. These electrons move so quickly in the regions around a stationary atom that during the time of an experiment they can be considered, by time averaging, to be represented by a constant electron distribution term. The value of this term is dependent on the species of atoms that are present in the structure. The second term is attributed to the slower vibrational motion of the atom and it's value is dependent on local interatomic forces, which, of course, vary from crystal to crystal and from position to position within the crystal. It will now be shown that the hot atomic scattering factor is the product of the cold atomic scattering factor, (the constant term due to the fast moving electrons for an atom at rest), with the Fourier transform of the p.d.f., (the term which describes the thermal motion of the atom), i.e. $f_j^h = f_j^c \mathcal{F}(P(\mathbf{r}))$.

Consider a small volume element, dV, containing $P(\mathbf{r})\,dV$ electrons, located at the end of the vector $\mathbf{r}$. Then the path of an X-ray of wavelength λ, travelling from its source to the detector, passing through the end point of $\mathbf{r}$, has increased by $\lambda \mathbf{r} \cdot \mathbf{s}$ over the path of an X-ray passing through the origin of the vector $\mathbf{r}$ (see Lipson and Cochran, 1953 p 3-7 for a diagram and discussion). If $\mathbf{s}_1$ is a vector parallel to the direction from the X-ray source to the end point of $\mathbf{r}$ and

$\mathbf{s_2}$ is a vector parallel to the direction from the origin of $\mathbf{r}$ to the detector, both of length $1/\lambda$, then $\mathbf{s}$ is defined as $\mathbf{s} = \mathbf{s}_1 - \mathbf{s}_2$. The change in the phase of an X-ray passing through the end point of $\mathbf{r}$ over an X-ray passing through the origin is this increase in distance, multiplied by the rate of change of phase with distance or $2\pi\mathbf{r} \cdot \mathbf{s}$ (Feynman *et al.*, 1977, chapter 29). The amplitude of wave, scattered from a point source at $\mathbf{r}$, is then proportional to $P(\mathbf{r})e^{2\pi i\mathbf{r}\cdot\mathbf{s}}\,dV$, where the proportionality constant is the cold scattering factor, f^c. The exponential term represents the decrease in intensity caused by a change in phase due to path difference. Since $P(\mathbf{r})$ is a continuous distribution, the amplitude of all the waves scattered by the distribution is found by the superposition principle to be

$$F(\mathbf{s}) = f^c \int_V P(\mathbf{r})e^{2\pi i\mathbf{r}\cdot\mathbf{s}}\,dV. \tag{2}$$

The integral in this equation is called the temperature factor. If there are many atoms, and hence many electron density functions, all contributing to the X-ray scattering, then the overall amplitude is the superposition of all these distributions,

$$\begin{aligned} F(\mathbf{s}) &= \sum_j^n \int_V f_j^c P_j(\mathbf{r}-\mathbf{r}_j)e^{2\pi i\mathbf{r}\cdot\mathbf{s}}\,dV \\ &= \sum_j^n \int_V f_j^c P_j(\mathbf{r}-\mathbf{r}_j)e^{2\pi i(\mathbf{r}-\mathbf{r}_j)\cdot\mathbf{s}}e^{2\pi i\mathbf{r}_j\cdot\mathbf{s}}\,dV \\ &\equiv \sum_j^n f_j^h(\mathbf{s})e^{2\pi i\mathbf{r}_j\cdot\mathbf{s}}. \end{aligned}$$

The hot atomic scattering factor is expressed as

$$f_j^h(\mathbf{s}) = f_j^c(\mathbf{s}) \int_V P_j(\mathbf{r})e^{2\pi i\mathbf{r}\cdot\mathbf{s}}\,dV = f_j^c(\mathbf{s})\mathcal{F}(P(\mathbf{r})),$$

where the temperature factor is the Fourier transform of the probability distribution function.

Isotropic Temperature Factor

As the first approximation under the harmonic model, it can be assumed that the vibrational amplitude of an atom is constant in all directions. This gives us an isotropic Gaussian probability distribution function of the form

$$P(\mathbf{r}) = \frac{1}{(\sqrt{2\pi\sigma^2})^3} e^{-r^2/2\sigma^2}$$

with zero mean and a root-mean-square deviation $\Delta r = \sigma$. Using spherical coordinates, the probability of finding an atom inside a sphere of radius r_o centered at the atom's equilibrium position is calculated by

$$\begin{aligned}
&\int_0^{2\pi}\int_0^{\pi}\int_0^{r_o} \frac{1}{(\sqrt{2\pi\sigma^2})^3} e^{-r^2/2\sigma^2} r^2 \sin\theta \, dr \, d\theta \, d\phi \\
&\quad = \frac{1}{\sigma^3}\sqrt{\frac{2}{\pi}} \int_0^{r_o} r^2 e^{-r^2/2\sigma^2} \, dr \\
&\quad = \mathrm{erf}(r_o/\sigma\sqrt{2}) \quad - \quad \sqrt{\frac{2}{\pi}}\frac{r_o}{\sigma} e^{-r_o^2/2\sigma^2}.
\end{aligned}$$

A sphere of radius $r_o = 1.5382\sigma$ encloses 50% of the probability density.

Once we have an expression for the p.d.f. we can calculate the form of the temperature factor under isotropic conditions (Willis and Pryor, 1975 p. 259 or Carpenter, 1969 p213). As shown in the last section, the temperature factor equals the Fourier transform of the p.d.f..

$$\begin{aligned}
\mathcal{F}(P(\mathbf{r})) &= \int_V P(\mathbf{r}) e^{2\pi i \mathbf{r}\cdot\mathbf{s}} \, dV \\
&= \int_0^{2\pi}\int_0^{\pi}\int_0^{\infty} \frac{1}{(\sqrt{2\pi\sigma^2})^3} e^{-r^2/2\sigma^2} e^{2\pi i \mathbf{r}\cdot\mathbf{s}} r^2 \sin\theta \, dr \, d\theta \, d\phi \\
&= \frac{2\pi}{(\sqrt{2\pi\sigma^2})^3} \int_0^{\pi}\int_0^{\infty} e^{-r^2/2\sigma^2} e^{2\pi i r s\cos\theta} r^2 \sin\theta \, dr \, d\theta.
\end{aligned}$$

This can be simplified with the trigonometric substitution:

$$u = 2\pi i r s \cos\theta \qquad du = -2\pi i r s \sin\theta \, d\theta,$$

from which we obtain

$$\begin{aligned}\mathcal{F}(P(\mathbf{r})) &= \frac{2\pi}{(\sqrt{2\pi\sigma^2})^3}\int_{-2\pi irs}^{2\pi irs}\int_0^\infty e^{-r^2/2\sigma^2}e^u r^2\,dr\,\frac{du}{2\pi irs}\\ &= \frac{2\pi}{(\sqrt{2\pi\sigma^2})^3}\int_0^\infty e^{-r^2/2\sigma^2}r^2\,dr\left(\frac{e^{2\pi irs}-e^{-2\pi irs}}{2i(\pi rs)}\right)\\ &= \frac{2}{s(\sqrt{2\pi\sigma^2})^3}\int_0^\infty e^{-r^2/2\sigma^2}r\sin 2\pi rs\,dr.\end{aligned}$$

This integral can be evaluated by separating it into parts:

$$u = \sin 2\pi rs \qquad dv = re^{-r^2/2\sigma^2}\,dr$$

$$du = 2\pi s\cos 2\pi rs\,dr \qquad v = -\sigma^2 e^{-r^2/2\sigma^2}$$

and from this:

$$\begin{aligned}\mathcal{F}(P(\mathbf{r})) &= \frac{2}{s(\sqrt{2\pi\sigma^2})^3}\left[-\sigma^2 e^{-r^2/2\sigma^2}\sin 2\pi rs\Big|_0^\infty + \int_0^\infty \sigma^2 e^{-r^2/2\sigma^2}2\pi s\cos 2\pi rs\,dr\right]\\ &= \frac{2\sigma^2 2\pi s}{s(\sqrt{2\pi\sigma^2})^3}\int_0^\infty e^{-r^2/2\sigma^2}\cos 2\pi rs\,dr.\end{aligned}$$

But

$$\int_0^\infty e^{-at^2}\cos 2xt\,dt = \frac{1}{2}\sqrt{\frac{\pi}{a}}\,e^{-x^2/a}.$$

Therefore

$$\begin{aligned}\mathcal{F}(P(\mathbf{r})) &= \frac{4\pi\sigma^2}{(\sqrt{2\pi\sigma^2})^3}\left[\frac{1}{2}\sqrt{2\pi\sigma^2}\,e^{-2\pi^2\sigma^2 s^2}\right]\\ &= e^{-2\pi^2\sigma^2 s^2}.\end{aligned}$$

One of the things observed from this calculation is that the Fourier transform of a Gaussian function is another Gaussian function with zero mean and root-mean-square deviation $\Delta s = 1/\sigma$, concluding that $\Delta r \cdot \Delta s = 1$.

Under the assumption of isotropic vibration, we obtain as the temperature factor

$$\mathcal{F}(P(\mathbf{r})) = e^{-2\pi^2\sigma^2 s^2}.$$

We calculate the structure factor using equation (1) and minimize the difference between the measured and calculated amplitudes by varying $\mathbf{r}_j$ and σ_j^2 for each of the j atoms in the unit cell.

Alternatively, note that $s^2 = 1/d^2$ so, from Bragg's equation

$$2d \sin\theta = \lambda,$$

we get

$$\mathcal{F}(P(\mathbf{r})) = e^{-8\pi^2\sigma^2 \frac{\sin^2\theta}{\lambda^2}}.$$

In order to save the trouble of carrying the $8\pi^2\sigma^2$ term around in the calculations define the isotropic temperature factor, B, as

$$B \equiv 8\pi^2\sigma^2.$$

We now have as our expression for the temperature factor

$$\mathcal{F}(P(\mathbf{r})) = e^{-B\frac{\sin^2\theta}{\lambda^2}}$$

and we minimize the difference between observed and calculated amplitudes by varying $\mathbf{r}_j$ and B instead of $\mathbf{r}_j$ and σ^2.

<u>Meaning of σ^2</u>. Let's take a closer look at the meaning of σ^2. It has been defined as the mean-square displacement of an atom from its equilibrium position. To

understand this, we calculate the radial mean-square displacement, $< r^2 >$.

$$
\begin{aligned}
< r^2 > &\equiv \int_V P(\mathbf{r}) r^2 \, dV \\
&= \int_V \frac{1}{(\sqrt{2\pi\sigma^2})^3} r^2 e^{-r^2/2\sigma^2} \, dV \\
&= \frac{1}{(\sqrt{2\pi\sigma^2})^3} \int_0^{2\pi} \int_0^{\pi} \int_0^{\infty} r^4 e^{-r^2/2\sigma^2} \sin\theta \, dr \, d\theta \, d\phi \\
&= \frac{2\pi}{(\sqrt{2\pi\sigma^2})^3} \int_0^{\pi} \int_0^{\infty} r^4 e^{-r^2/2\sigma^2} \sin\theta \, dr \, d\theta \\
&= \frac{4\pi}{(\sqrt{2\pi\sigma^2})^3} \int_0^{\infty} r^4 e^{-r^2/2\sigma^2} \, dr \\
&= \frac{4\pi}{(\sqrt{2\pi\sigma^2})^3} \left[\frac{3}{8} (2\sigma^2)^2 \sqrt{2\pi\sigma^2} \right] \\
&= 3\sigma^2.
\end{aligned}
$$

Here we made use of the integral $\int_0^{\infty} t^{2n} e^{-at^2} \, dt = \frac{(2n-1)!!}{2^{n+1} a^n} \sqrt{\frac{\pi}{a}}$ (Abramowitz and Stegun, 1972). The average mean-square displacement of an atom over all space, from its equilibrium position, is $< r^2 >= 3\sigma^2$. If we examine $< x^2 >$, which is the mean-square displacement projected along the x direction we find

$$
\begin{aligned}
< x^2 > &\equiv \int_V P(\mathbf{r}) x^2 \, dV \\
&= \int_V \frac{1}{(\sqrt{2\pi\sigma^2})^3} x^2 e^{-r^2/2\sigma^2} \, dV \\
&= \frac{1}{(\sqrt{2\pi\sigma^2})^3} \int_{-\infty}^{\infty} \int_{-\infty}^{\infty} \int_{-\infty}^{\infty} x^2 e^{-x^2/2\sigma^2} e^{-y^2/2\sigma^2} e^{-z^2/2\sigma^2} \, dx \, dy \, dz \\
&= \frac{1}{(\sqrt{2\pi\sigma^2})^2} \int_{-\infty}^{\infty} \int_{-\infty}^{\infty} x^2 e^{-x^2/2\sigma^2} e^{-y^2/2\sigma^2} \, dx \, dy \\
&= \frac{1}{\sqrt{2\pi\sigma^2}} \int_{-\infty}^{\infty} x^2 e^{-x^2/2\sigma^2} \, dx \\
&= \frac{2}{\sqrt{2\pi\sigma^2}} \int_0^{\infty} x^2 e^{-x^2/2\sigma^2} \, dx \\
&= \frac{2}{\sqrt{2\pi\sigma^2}} \left[\frac{2\sigma^2}{4} \sqrt{2\pi\sigma^2} \right] \\
&= \sigma^2.
\end{aligned}
$$

Then, for an isotropic p.d.f. $< y^2 >=< z^2 >=< x^2 >= \sigma^2$. If $< x^2 >$, $< y^2 >$, and $< z^2 >$ are measured along orthonormal axes then

$$< r^2 >=< x^2 > + < y^2 > + < z^2 >= 3\sigma^2.$$

$< x^2 >$ is a projection operator: the magnitude of vibration in the x direction is greater than $< x^2 >$.

Anisotropic Temperature Factor

As a second approximation under the harmonic model, it can be assumed that an atom's vibrational displacement varies with direction. The probability distribution function takes the form of an anisotropic Gaussian function:

$$P(\mathbf{r}) = \frac{1}{(2\pi)^{3/2}(\sigma_1\sigma_2\sigma_3)} \exp\left(-1/2[\mathbf{r}]_C^t \begin{bmatrix} 1/\sigma_1^2 & 0 & 0 \\ 0 & 1/\sigma_2^2 & 0 \\ 0 & 0 & 1/\sigma_3^2 \end{bmatrix} [\mathbf{r}]_C\right).$$

This is expressed with respect to the Cartesian basis C=$\{\mathbf{i},\mathbf{j},\mathbf{k}\}$ coincident with the principal axes of the ellipsoid. Letting $[\mathbf{r}]_C^t = [\,x_1 \quad x_2 \quad x_3\,]$ and $[\mathbf{s}]_C^t = [\,s_1 \quad s_2 \quad s_3\,]$, then as shown earlier, we obtain the temperature factor by taking the Fourier transform of the probability distribution function

$$\begin{aligned}
\mathcal{F}(P(\mathbf{r})) &= \int_V P(\mathbf{r}) e^{2\pi i \mathbf{r}\cdot\mathbf{s}}\, dV \\
&= \frac{1}{(2\pi)^{3/2}(\sigma_1\sigma_2\sigma_3)} \int_V e^{-(\frac{x_1^2}{2\sigma_1^2}+\frac{x_2^2}{2\sigma_2^2}+\frac{x_3^2}{2\sigma_3^2})} e^{(2\pi i \mathbf{r}\cdot\mathbf{s})}\, dV \\
&= \prod_{i=1}^{3} \frac{1}{(2\pi\sigma_i^2)^{1/2}} \int_{-\infty}^{\infty} e^{(-\frac{x_i^2}{2\sigma_i^2}+2\pi i x_i s_i)}\, dx_i \\
&= \prod_{i=1}^{3} \frac{e^{-2\pi^2\sigma_i^2 s_i^2}}{(2\pi\sigma_i^2)^{1/2}} \int_{-\infty}^{\infty} e^{-(\frac{x_i}{\sqrt{2}\sigma_i}-\sqrt{2}\pi i\sigma_i s_i)^2}\, dx_i \\
&= \prod_{i=1}^{3} e^{-2\pi^2\sigma_i^2 s_i^2} \\
&= \exp\left(-2\pi^2[\mathbf{s}]_C^t \begin{bmatrix} \sigma_1^2 & 0 & 0 \\ 0 & \sigma_2^2 & 0 \\ 0 & 0 & \sigma_3^2 \end{bmatrix} [\mathbf{s}]_C\right).
\end{aligned}$$

Next we need to transform the exponent to the D^* basis since it would be awkward to express all the vectors in the crystal with respect to the principal axes of one of the atoms. Let $[\mathbf{s}]^t_{D^*} = [\,h \quad k \quad l\,]$ and let M be the matrix such that $M[\mathbf{s}]_{D^*} = [\mathbf{s}]_C$. Then

$$M[\mathbf{a}^*]_{D^*} = [\mathbf{a}^*]_C \qquad \text{giving the first column of M,}$$

$$M[\mathbf{b}^*]_{D^*} = [\mathbf{b}^*]_C \qquad \text{giving the second column of M,}$$

$$M[\mathbf{c}^*]_{D^*} = [\mathbf{c}^*]_C \qquad \text{giving the third column of M.}$$

Note that M is not unique but will be different for every translationally non-equivalent atom. Hence

$$\begin{aligned}
M &= [\,[\mathbf{a}^*]_C \quad [\mathbf{b}^*]_C \quad [\mathbf{c}^*]_C\,] \\
&= \begin{bmatrix} \mathbf{i}\cdot\mathbf{a}^* & \mathbf{i}\cdot\mathbf{b}^* & \mathbf{i}\cdot\mathbf{c}^* \\ \mathbf{j}\cdot\mathbf{a}^* & \mathbf{j}\cdot\mathbf{b}^* & \mathbf{j}\cdot\mathbf{c}^* \\ \mathbf{k}\cdot\mathbf{a}^* & \mathbf{k}\cdot\mathbf{b}^* & \mathbf{k}\cdot\mathbf{c}^* \end{bmatrix} \\
&= \begin{bmatrix} a^*\cos(\mathbf{a}^*\wedge\mathbf{i}) & b^*\cos(\mathbf{b}^*\wedge\mathbf{i}) & c^*\cos(\mathbf{c}^*\wedge\mathbf{i}) \\ a^*\cos(\mathbf{a}^*\wedge\mathbf{j}) & b^*\cos(\mathbf{b}^*\wedge\mathbf{j}) & c^*\cos(\mathbf{c}^*\wedge\mathbf{j}) \\ a^*\cos(\mathbf{a}^*\wedge\mathbf{k}) & b^*\cos(\mathbf{b}^*\wedge\mathbf{k}) & c^*\cos(\mathbf{c}^*\wedge\mathbf{k}) \end{bmatrix} \\
&= \begin{bmatrix} \cos(\mathbf{a}^*\wedge\mathbf{i}) & \cos(\mathbf{b}^*\wedge\mathbf{i}) & \cos(\mathbf{c}^*\wedge\mathbf{i}) \\ \cos(\mathbf{a}^*\wedge\mathbf{j}) & \cos(\mathbf{b}^*\wedge\mathbf{j}) & \cos(\mathbf{c}^*\wedge\mathbf{j}) \\ \cos(\mathbf{a}^*\wedge\mathbf{k}) & \cos(\mathbf{b}^*\wedge\mathbf{k}) & \cos(\mathbf{c}^*\wedge\mathbf{k}) \end{bmatrix} \begin{bmatrix} a^* & 0 & 0 \\ 0 & b^* & 0 \\ 0 & 0 & c^* \end{bmatrix} \\
&= CD
\end{aligned}$$

defining both C and D. The temperature factor, then, is expressed

$$\begin{aligned}
\mathcal{F}(P(\mathbf{r})) &= \exp\left(-2\pi^2[\mathbf{s}]^t_C \begin{bmatrix} \sigma_1^2 & 0 & 0 \\ 0 & \sigma_2^2 & 0 \\ 0 & 0 & \sigma_3^2 \end{bmatrix} [\mathbf{s}]_C\right) \\
&= \exp\left(-2\pi^2(CD[\mathbf{s}]_{D^*})^t \begin{bmatrix} \sigma_1^2 & 0 & 0 \\ 0 & \sigma_2^2 & 0 \\ 0 & 0 & \sigma_3^2 \end{bmatrix} CD[\mathbf{s}]_{D^*}\right) \\
&= \exp\left(-2\pi^2[\mathbf{s}]^t_{D^*} D^t C^t \begin{bmatrix} \sigma_1^2 & 0 & 0 \\ 0 & \sigma_2^2 & 0 \\ 0 & 0 & \sigma_3^2 \end{bmatrix} CD[\mathbf{s}]_{D^*}\right).
\end{aligned}$$

If U is defined as

$$U = C^t \begin{bmatrix} \sigma_1^2 & 0 & 0 \\ 0 & \sigma_2^2 & 0 \\ 0 & 0 & \sigma_3^2 \end{bmatrix} C,$$

then we obtain the familiar temperature factor expression

$$\begin{aligned}\mathcal{F}(P(\mathbf{r})) &= e^{-2\pi^2[\mathbf{s}]_D^t \cdot D^t U D [\mathbf{s}]_D \cdot} \\ &= \exp(-2\pi^2(U_{11}a^{*2}h^2 + U_{22}b^{*2}k^2 + U_{33}c^{*2}l^2 \\ &\quad + 2U_{12}a^*b^*hk + 2U_{13}a^*c^*hl + 2U_{23}b^*c^*kl)).\end{aligned}$$

The U_{ij}'s are defined as

$$\begin{aligned}U_{11} &= \sigma_1^2\cos^2(\mathbf{a}^* \wedge \mathbf{i}) + \sigma_2^2\cos^2(\mathbf{a}^* \wedge \mathbf{j}) + \sigma_3^2\cos^2(\mathbf{a}^* \wedge \mathbf{k}) \\ U_{22} &= \sigma_1^2\cos^2(\mathbf{b}^* \wedge \mathbf{i}) + \sigma_2^2\cos^2(\mathbf{b}^* \wedge \mathbf{j}) + \sigma_3^2\cos^2(\mathbf{b}^* \wedge \mathbf{k}) \\ U_{33} &= \sigma_1^2\cos^2(\mathbf{c}^* \wedge \mathbf{i}) + \sigma_2^2\cos^2(\mathbf{c}^* \wedge \mathbf{j}) + \sigma_3^2\cos^2(\mathbf{c}^* \wedge \mathbf{k}) \\ U_{12} = U_{21} &= \sigma_1^2\cos(\mathbf{a}^* \wedge \mathbf{i})\cos(\mathbf{b}^* \wedge \mathbf{i}) + \sigma_2^2\cos(\mathbf{a}^* \wedge \mathbf{j})\cos(\mathbf{b}^* \wedge \mathbf{j}) \\ &\quad + \sigma_3^2\cos(\mathbf{a}^* \wedge \mathbf{k})\cos(\mathbf{b}^* \wedge \mathbf{k}) \\ U_{13} = U_{31} &= \sigma_1^2\cos(\mathbf{a}^* \wedge \mathbf{i})\cos(\mathbf{c}^* \wedge \mathbf{i}) + \sigma_2^2\cos(\mathbf{a}^* \wedge \mathbf{j})\cos(\mathbf{c}^* \wedge \mathbf{j}) \\ &\quad + \sigma_3^2\cos(\mathbf{a}^* \wedge \mathbf{k})\cos(\mathbf{c}^* \wedge \mathbf{k}) \\ U_{23} = U_{32} &= \sigma_1^2\cos(\mathbf{b}^* \wedge \mathbf{i})\cos(\mathbf{c}^* \wedge \mathbf{i}) + \sigma_2^2\cos(\mathbf{b}^* \wedge \mathbf{j})\cos(\mathbf{c}^* \wedge \mathbf{j}) \\ &\quad + \sigma_3^2\cos(\mathbf{b}^* \wedge \mathbf{k})\cos(\mathbf{c}^* \wedge \mathbf{k}).\end{aligned}$$

Now, define the matrix β as $\beta = 2\pi^2(D^tUD)$, then

$$\begin{aligned}\beta_{11} &= 2\pi^2 U_{11}a^{*2} \\ \beta_{22} &= 2\pi^2 U_{22}b^{*2} \\ \beta_{33} &= 2\pi^2 U_{33}c^{*2} \\ \beta_{12} = \beta_{21} &= 2\pi^2 U_{12}a^*b^* \\ \beta_{13} = \beta_{31} &= 2\pi^2 U_{13}a^*c^* \\ \beta_{23} = \beta_{32} &= 2\pi^2 U_{23}b^*c^*.\end{aligned}$$

In summary, we have two expressions commonly used for the temperature factor:

$$\begin{aligned}\mathcal{F}(P(\mathbf{r})) &= e^{-2\pi^2[\mathbf{s}]^t_{D^*}(D^tUD)[\mathbf{s}]_{D^*}} \\ &= \exp(-2\pi^2(U_{11}a^{*2}h^2 + U_{22}b^{*2}k^2 + U_{33}c^{*2}l^2 \\ &\qquad + 2U_{12}a^*b^*hk + 2U_{13}a^*c^*hl + 2U_{23}b^*c^*kl)) \\ &= \exp(\beta_{11}h^2 + \beta_{22}k^2 + \beta_{33}l^2 + 2\beta_{12}hk + 2\beta_{13}hl + 2\beta_{23}kl) \\ &= e^{-[\mathbf{s}]^t_{D^*}\beta[\mathbf{s}]_{D^*}}\end{aligned}$$

The latter term is often used in least squares refinements because of its simplicity, but care must be taken when reading the literature since some authors include the factor of 2 in the β_{ij} terms.

Symmetry Constraints

If two atoms are related by some symmetry operation, α, then their thermal ellipsoids must also be related by the symmetry operation. Examine this relation for the β matrix. First, note that the translational part of a symmetry operation will not affect the values of the β_{ij}'s. Let $M_D(\alpha)$ be the matrix representation of the point symmetry operation with respect to the direct basis and $M_{D^*}(\alpha)$ be the representation with respect to the reciprocal basis. Then $M_D(\alpha) = M^{-t}_{D^*}(\alpha)$. (Boisen and Gibbs, 1985 p.60) Also, let $M_{D^*}(\alpha)[\mathbf{s}]_{D^*} = [\mathbf{s}']_{D^*}$, where $\mathbf{s}'$ is the transformed vector and let β' be the transformed β matrix. Then

$$\begin{aligned}[\mathbf{s}']^t_{D^*}\beta'[\mathbf{s}']_{D^*} &= [\mathbf{s}]^t_{D^*}\beta[\mathbf{s}]_{D^*} \\ &= (M^-_{D^*}(\alpha)[\mathbf{s}']_{D^*})^t\beta(M^-_{D^*}(\alpha)[\mathbf{s}']_{D^*}) \\ &= [\mathbf{s}']^t_{D^*}\left(M^{-t}_{D^*}(\alpha)\beta M^-_{D^*}(\alpha)\right)[\mathbf{s}']_{D^*}.\end{aligned}$$

Since this is true for any vector, $\mathbf{s}$, we can conclude that

$$\begin{aligned}\beta' &= M^{-t}_{D^*}(\alpha)\beta M^-_{D^*}(\alpha) \\ &= M_D(\alpha)\beta M^t_D(\alpha).\end{aligned}$$

When atoms are known to be in special positions then the temperature factor matrix may reduce to a constrained form. If this is not taken into consideration in a least squares refinement then singular temperature factor matrices are often the result. This form can be deduced by letting β' be set equal to β in the above expression to obtain the constraint condition $\beta = M_D(\alpha)\beta M_D^t(\alpha)$.

For example, the garnets belong to space group $Ia3d$ and the general chemical structural formula is $X_3[Y_2](Z_3)O_{12}$ with eight formula units per cell (Novak and Gibbs, 1971). The X cation is in special position c which has 222 point symmetry. The Y cation is in special position a which has $\bar{3}$ point symmetry. The Z cation is in special position d which has $\bar{4}$ point symmetry, and the oxygen is in a general position. The temperature factor matrix for the oxygen atom is a general β matrix. Now examine the matrix for the Z cation. The position of the Z cation is $[3/8 \quad 0 \quad 1/4]^t$ so that a matrix which leaves this point translationally invariant is

$$\begin{bmatrix} -1 & 0 & 0 & 3/4 \\ 0 & 0 & 1 & 3/4 \\ 0 & -1 & 0 & 1/4 \\ 0 & 0 & 0 & 1 \end{bmatrix}$$

Extracting the point symmetry part of the matrix, we find that

$$M\beta M^t = \begin{bmatrix} -1 & 0 & 0 \\ 0 & 0 & 1 \\ 0 & -1 & 0 \end{bmatrix} \begin{bmatrix} \beta_{11} & \beta_{12} & \beta_{13} \\ \beta_{12} & \beta_{22} & \beta_{23} \\ \beta_{13} & \beta_{23} & \beta_{33} \end{bmatrix} \begin{bmatrix} -1 & 0 & 0 \\ 0 & 0 & -1 \\ 0 & 1 & 0 \end{bmatrix}$$

$$= \begin{bmatrix} \beta_{11} & -\beta_{13} & \beta_{12} \\ -\beta_{13} & \beta_{33} & -\beta_{23} \\ \beta_{12} & -\beta_{23} & \beta_{22} \end{bmatrix}.$$

This is the form of the β matrix when transformed by a $\bar{4}$ symmetry operation. To find the constraint imposed by the special position we solve

$$\begin{bmatrix} \beta_{11} & \beta_{12} & \beta_{13} \\ \beta_{12} & \beta_{22} & \beta_{23} \\ \beta_{13} & \beta_{23} & \beta_{33} \end{bmatrix} = \begin{bmatrix} \beta_{11} & -\beta_{13} & \beta_{12} \\ -\beta_{13} & \beta_{33} & -\beta_{23} \\ \beta_{12} & -\beta_{23} & \beta_{22} \end{bmatrix}.$$

The temperature factor matrix must be of the form

$$\begin{bmatrix} \beta_{11} & 0 & 0 \\ 0 & \beta_{22} & 0 \\ 0 & 0 & \beta_{22} \end{bmatrix}.$$

Examine the Y cation. Its position is $[0 \quad 0 \quad 0]^t$ so we need only find a matrix which leaves this position invariant and since the point symmetry is $\bar{3}$, then choose, say,

$$M = \begin{bmatrix} 0 & 1 & 0 \\ 0 & 0 & 1 \\ 1 & 0 & 0 \end{bmatrix}$$

to get

$$\begin{bmatrix} \beta_{11} & \beta_{12} & \beta_{12} \\ \beta_{12} & \beta_{11} & \beta_{12} \\ \beta_{12} & \beta_{12} & \beta_{11} \end{bmatrix}$$

The X cation is in a special position, $[1/8 \quad 0 \quad 1/4]^t$, with point symmetry 222, which has two generating matrices, so we need to use both of them to obtain the form of our temperature factor matrix. We can use (each in turn)

$$M = \begin{bmatrix} 1 & 0 & 0 \\ 0 & -1 & 0 \\ 0 & 0 & -1 \end{bmatrix} \quad \text{and} \quad M = \begin{bmatrix} -1 & 0 & 0 \\ 0 & 0 & -1 \\ 0 & -1 & 0 \end{bmatrix}$$

and we find that our temperature factor matrix should be of the form

$$\beta = \begin{bmatrix} \beta_{11} & 0 & 0 \\ 0 & \beta_{22} & \beta_{23} \\ 0 & \beta_{23} & \beta_{22} \end{bmatrix}$$

A completed list of the constrained forms is given in the paper by Peterse and Palm (1965).

Mean-Square Displacements Along Vectors

To obtain an expression for the mean-square displacement, $< \mu_{\mathbf{v}}^2 >$, of an atom as projected along some specified vector, $\mathbf{v}$, assume a cartesian basis, $C = \{\mathbf{i}, \mathbf{j}, \mathbf{k}\}$, coincident with the principal axes of the ellipsoid (Nelmes, 1969). Let

$[\mathbf{v}]_C^t = [\,v_1 \quad v_2 \quad v_3\,]$ and $[\mathbf{r}]_C^t = [\,x_1 \quad x_2 \quad x_3\,]$ then

$$
\begin{aligned}
<\mu_{\mathbf{v}}^2> &= \int_V (\frac{\mathbf{v}}{\|\mathbf{v}\|} \cdot \mathbf{r})^2 P(\mathbf{r}) dV \\
&= \frac{1}{(2\pi)^{3/2}(\sigma_1\sigma_2\sigma_3)\|\mathbf{v}\|^2} \int_V (\mathbf{v}\cdot\mathbf{r})^2 e^{-(\frac{x_1^2}{2\sigma_1^2}+\frac{x_2^2}{2\sigma_2^2}+\frac{x_3^2}{2\sigma_3^2})} dV \\
&= \frac{1}{(2\pi)^{3/2}(\sigma_1\sigma_2\sigma_3)\|\mathbf{v}\|^2} \int_{-\infty}^{\infty}\int_{-\infty}^{\infty}\int_{-\infty}^{\infty} (v_1^2x_1^2 + v_2^2x_2^2 + v_3^2x_3^2 + 2v_1v_2x_1x_2 \\
&\qquad + 2v_1v_3x_1x_3 + 2v_2v_3x_2x_3) e^{-(\frac{x_1^2}{2\sigma_1^2}+\frac{x_2^2}{2\sigma_2^2}+\frac{x_3^2}{2\sigma_3^2})} dx_1\,dx_2\,dx_3 \\
&= \frac{1}{\|\mathbf{v}\|^2}(v_1^2\sigma_1^2 + v_2^2\sigma_2^2 + v_3^2\sigma_3^2) \\
&= \frac{1}{\|\mathbf{v}\|^2}\left([\mathbf{v}]_C^t \begin{bmatrix} \sigma_1^2 & 0 & 0 \\ 0 & \sigma_2^2 & 0 \\ 0 & 0 & \sigma_3^2 \end{bmatrix} [\mathbf{v}]_C\right) \\
&= \frac{[\mathbf{v}]_{D^*}^t D^t U D [\mathbf{v}]_{D^*}}{[\mathbf{v}]_{D^*}^t G^* [\mathbf{v}]_{D^*}} \\
&= \frac{(GG^*[\mathbf{v}]_{D^*}^t)D^tUD(GG^*[\mathbf{v}]_{D^*})}{(GG^*[\mathbf{v}]_{D^*}^t)G^*(GG^*[\mathbf{v}]_{D^*})} \\
&= \frac{[\mathbf{v}]_D^t(G^tD^tUDG)[\mathbf{v}]_D}{[\mathbf{v}]_D^t G[\mathbf{v}]_D} \\
&= \frac{[\mathbf{v}]_D^t(G^t\beta G)[\mathbf{v}]_D}{2\pi^2[\mathbf{v}]_D^t G[\mathbf{v}]_D}. \qquad (3)
\end{aligned}
$$

The last two expressions are used for computations.

Principal Axes

It is of interest to determine the length and orientation of the principal axes of a thermal ellipsoid. Since the probability ellipsoid is of the quadratic form $1/2\mathbf{x}^t\Lambda\mathbf{x}$ where Λ may be diagonalized to

$$\Lambda = \begin{bmatrix} \frac{1}{\sigma_1^2} & 0 & 0 \\ 0 & \frac{1}{\sigma_2^2} & 0 \\ 0 & 0 & \frac{1}{\sigma_3^2} \end{bmatrix},$$

then the lengths of the principal axes must be σ_1, σ_2 and σ_3 (Franklin, 1968 p.94).

We can obtain these three optimum values of σ by considering Equation 3

$$< \mu_{\mathbf{v}}^2 >= \frac{[\mathbf{v}]_D^t (G^t \beta G)[\mathbf{v}]_D}{2\pi^2 [\mathbf{v}]_D^t G[\mathbf{v}]_D}.$$

Note that this discussion will use the β form of the thermal ellipsoid, however the method applies equally well to the U form (see Waser, 1955 or Busing and Levy, 1958). Take the derivative of $< \mu_{\mathbf{v}}^2 >$ with respect to the vector $\mathbf{v}$, and set it to zero.

$$\frac{d < \mu_{\mathbf{v}}^2 >}{d\mathbf{v}} = \frac{(2G^t \beta G[\mathbf{v}]_D)(2\pi^2 [\mathbf{v}]_D^t G[\mathbf{v}]_D) - (4\pi^2 G[\mathbf{v}]_D)([\mathbf{v}]_D^t G^t \beta G[\mathbf{v}]_D)}{(2\pi^2 [\mathbf{v}]_D^t G[\mathbf{v}]_D)^2} = 0.$$

Then

$$\begin{aligned}
(2G^t \beta G[\mathbf{v}]_D)(2\pi^2 [\mathbf{v}]_D^t G[\mathbf{v}]_D) &= (4\pi^2 G[\mathbf{v}]_D)([\mathbf{v}]_D^t G^t \beta G[\mathbf{v}]_D) \\
(2G^t \beta G[\mathbf{v}]_D) &= (4\pi^2 G[\mathbf{v}]_D) \frac{([\mathbf{v}]_D^t G^t \beta G[\mathbf{v}]_D)}{(2\pi^2 [\mathbf{v}]_D^t G[\mathbf{v}]_D)} \\
&= 4\pi^2 \sigma^2 G[\mathbf{v}]_D \\
\beta G[\mathbf{v}]_D &= \lambda [\mathbf{v}]_D, \qquad \text{where} \qquad \lambda = 2\pi^2 \sigma^2.
\end{aligned}$$

The root-mean square displacements parallel to the principal axes of the ellipsoid are the solutions to the equation $\sigma = \sqrt{\frac{\lambda}{2\pi^2}}$ for the three eigenvalues of βG. The eigenvectors are parallel to the principal axes and are expressed in direct space.

As an example, consider the thermal ellipsoid for Si1 in coesite (Geisinger, 1987). The cell parameters are:

$$a = 7.1367 \qquad b = 12.3695 \qquad c = 7.1742 \qquad \beta = 120.337°.$$

The U matrix is

$$U = \begin{bmatrix} .0055 & -.0010 & .0027 \\ -.0010 & .0046 & -.0006 \\ .0027 & -.0006 & .0051 \end{bmatrix}.$$

Using the relation $\beta = 2\pi^2 (D^t U D)$ we construct the β matrix. Then

$$\begin{aligned}
\beta G &= \begin{bmatrix} .00268 & -.00027 & .00134 \\ -.00027 & .00055 & -.00018 \\ .00134 & -.00018 & .00249 \end{bmatrix} \begin{bmatrix} 50.93249 & .00000 & -25.86041 \\ .00000 & 153.00435 & .00000 \\ -25.86041 & .00000 & 51.46915 \end{bmatrix} \\
&= \begin{bmatrix} .101846 & -.041311 & -.000337 \\ -.009097 & .084152 & -.002282 \\ .003857 & -.027541 & .093505 \end{bmatrix}
\end{aligned}$$

The eigenvalues are

$$.115447 \qquad .070052 \qquad .094005$$

and the eigenvectors are

$$\begin{bmatrix} .13428 \\ -.04486 \\ .07991 \end{bmatrix} \quad \begin{bmatrix} .08774 \\ .06701 \\ .06425 \end{bmatrix} \quad \begin{bmatrix} -.02505 \\ -.00577 \\ .12477 \end{bmatrix}.$$

The root mean square length of the axes are

$$.076 \qquad .060 \qquad .069.$$

We see that the principal axes define an ellipse which is fairly spherical. This is common to Si atoms in tetrahedral coordination under the harmonic approximation.

To further define the eigenvectors, many authors publish their orientations with respect to the direct crystal basis. For this Si atom we find

$$\angle(\mathbf{v}_1 \wedge \mathbf{a}) = 48^\circ \qquad \angle(\mathbf{v}_1 \wedge \mathbf{b}) = 56^\circ \qquad \angle(\mathbf{v}_1 \wedge \mathbf{c}) = 85^\circ$$

$$\angle(\mathbf{v}_2 \wedge \mathbf{a}) = 67^\circ \qquad \angle(\mathbf{v}_2 \wedge \mathbf{b}) = 34^\circ \qquad \angle(\mathbf{v}_2 \wedge \mathbf{c}) = 82^\circ$$

$$\angle(\mathbf{v}_3 \wedge \mathbf{a}) = 51^\circ \qquad \angle(\mathbf{v}_3 \wedge \mathbf{b}) = 86^\circ \qquad \angle(\mathbf{v}_3 \wedge \mathbf{c}) = 10^\circ.$$

Cross-Sections of the Ellipsoids

Calculations to obtain thermal corrected bond lengths (Busing and Levy, 1964) need the mean-square displacement of an atom in the plane perpendicular to a given bond vector. Given the vector between any two bonded atoms, $\mathbf{v}$, we can calculate the vibration along the bond using Equation 3,

$$< u^2 >= \frac{[\mathbf{v}]_D^t (G^t D^t U D G)[\mathbf{v}]_D}{[\mathbf{v}]_D^t G[\mathbf{v}]_D} = \frac{[\mathbf{v}]_D^t (G^t \beta G)[\mathbf{v}]_D}{2\pi^2 [\mathbf{v}]_D^t G[\mathbf{v}]_D}.$$

The mean square displacement for the atom, over all space, is the sum of the displacements along the principal axes of the ellipse and hence can be expressed

$$< r^2 >= \sigma_1^2 + \sigma_2^2 + \sigma_3^2 = \frac{trace(\beta G)}{2\pi^2}.$$

If we imagine a change of basis such that the bond vector coincides with one of the new basis axes, then by invariance of the trace under similarity transformations, the isotropic mean-square displacement of the atom in a plane perpendicular to the bond vector is

$$< r'^2 >= \frac{trace(\beta G)}{2\pi^2} - < u^2 > .$$

Using this method we lose the anisotropic information about the shape and orientation of the cross-section. To get this information let $\mathbf{v}$ be any vector which is perpendicular to the desired cross-section, where $[\mathbf{v}]_D^t = [\, v_1 \quad v_2 \quad v_3 \,]$ with respect to the direct basis and $[\mathbf{v}]_{D^*}^t = (G[\mathbf{v}]_D)^t = [\, v_1^* \quad v_2^* \quad v_3^* \,]$ with respect to the reciprocal basis. If $\mathbf{x}$ ($[\mathbf{x}]_D^t = [\, x_1 \quad x_2 \quad x_3 \,]$) is any vector in the cross-section, then the equation

$$\mathbf{x} \cdot \mathbf{v} = [\mathbf{x}]_D^t G[\mathbf{v}]_D = [\mathbf{x}]_D^t [\mathbf{v}]_{D^*} = x_1 v_1^* + x_2 v_2^* + x_3 v_3^* = 0$$

must be satisfied. Suppose $\mathbf{q}$ and $\mathbf{r}$ are any two non-collinear vectors satisfying this equation. Then we can obtain the elliptic cross-section by transforming the ellipsoid to the constrained plane using a transformation matrix, T, with $[\mathbf{q}]_D$ and $[\mathbf{r}]_D$ as its columns,

$$T = [\, [\mathbf{q}]_D \quad [\mathbf{r}]_D \,] .$$

T will transform a vector from the plane, written with respect to the basis $D' = \{\mathbf{q}, \mathbf{r}\}$, to our three dimensional direct space. If v_3^* were not zero then $\mathbf{q}$ and $\mathbf{r}$ could be chosen as follows. A solution for x_3 could be written in terms of x_1 and x_2 as

$$x_3 = -\frac{v_1^*}{v_3^*} x_1 - \frac{v_2^*}{v_3^*} x_2 .$$

Choosing $x_1 = 1$ and $x_2 = 0$ for $\mathbf{q}$ and $x_1 = 0$ and $x_2 = 1$ for $\mathbf{r}$ we obtain a

transformation equation

$$T[\mathbf{x}]_{D'} = \begin{bmatrix} 1 & 0 \\ 0 & 1 \\ -\frac{v_1^*}{v_3^*} & -\frac{v_2^*}{v_3^*} \end{bmatrix} \begin{bmatrix} x_1 \\ x_2 \end{bmatrix} = \begin{bmatrix} x_1 \\ x_2 \\ x_3 \end{bmatrix} = [\mathbf{x}]_D.$$

Any choice of non-collinear $\mathbf{q}$ and $\mathbf{r}$ is theoretically satisfactory, however for computational purposes, in which numerical instability may be a problem, it may be best to choose them to be orthonormal.

After the transformation matrix has been chosen we can then obtain an expression for displacements in the plane.

$$\begin{aligned} < u^2 > &= \frac{[\mathbf{x}]_D^t G^t \beta G [\mathbf{x}]_D}{2\pi^2 [\mathbf{x}]_D^t G [\mathbf{x}]_D} \\ &= \frac{(T[\mathbf{x}]_{D'})^t G^t \beta G (T[\mathbf{x}]_{D'})}{2\pi^2 (T[\mathbf{x}]_{D'})^t G (T[\mathbf{x}]_{D'})} \\ &= \frac{[\mathbf{x}]_{D'} T^t G^t \beta G T [\mathbf{x}]_{D'}}{2\pi^2 [\mathbf{x}]_{D'} T^t G T [\mathbf{x}]_{D'}}. \end{aligned}$$

To obtain the principal axes of this ellipse and the associated eigenvalues we solve the generalized eigenvalue problem (Franklin, 1968)

$$T^t G^t \beta G T [\mathbf{x}]_{D'} = \lambda T^t G T [\mathbf{x}]_{D'}.$$

$[\mathbf{x}_i]_{D'}^t = [\, x'_{1i} \quad x'_{2i} \,]$ are the eigenvectors and $\lambda_i = 2\pi^2 \sigma'^2_i$ are the two eigenvalues. It follows that in direct space the principal axes of the ellipse perpendicular to the vector $\mathbf{v}$ are $T[\mathbf{x}_i]_{D'}$ In addition, it is found that

$$< r'^2 > = \frac{trace(\beta G)}{2\pi^2} - < u^2 > = \sigma'^2_1 + \sigma'^2_2.$$

Isotropic Equivalent to the Anisotropic Temperature Factor

In some instances it is of use to know the isotropic temperature factor which would be equivalent to the anisotropic one. This isotropic factor usually is not the one that would be obtained from the least squares refinement but can be

considered a good estimate. In practice, assume that the isotropic equivalent mean-square displacement is equal to the average of the mean-square displacements along the principal axis of the anisotropic thermal ellipsoid. Recalling that $\lambda_i = 2\pi^2\sigma_i^2$ were the eigenvalue of βG, and that the trace of this matrix is invariant under a similarity transformation, then the average eigenvalue of βG is $1/3$ trace(βG). Hence the average mean square displacement is

$$< \sigma^2 >= \frac{1}{3 \cdot 2\pi^2} tr(\beta G).$$

The equivalent isotropic temperature factor is then

$$\begin{aligned} \bar{B} &= 8\pi^2 < \sigma^2 > \\ &= \frac{4}{3} tr(\beta G) \\ &= \frac{4}{3} tr(2\pi^2 D^t U D G) = \frac{8\pi^2}{3} tr(D^t U D G) \\ &= \frac{4}{3} \sum_{i=1}^{3} \sum_{j=1}^{3} \beta_{ij} G_{ij} \qquad \text{(Hamilton, 1959).} \end{aligned} \tag{4}$$

Note that there has been some misunderstanding in many papers about how to calculate this factor when the anisotropic factors have been presented as the U matrix. They use the expression $\bar{B} = \frac{8\pi^2}{3} trace(U)$, but this is only true for orthogonal bases.

As an example, we can calculate the isotropic temperature factor for the Si1 atom in coesite (Geisinger, 1987)

$$\begin{aligned} \bar{B} &= \frac{4}{3} tr(\beta G) \\ &= \frac{4}{3}(.101846 + .084152 + .093505) \\ &= .373 \end{aligned}$$

As a check, we can take the average from the root mean square lengths (these are

calculated in the section on Principal Axes).

$$\bar{B} = 8\pi^2 < \sigma^2 >$$
$$= 8\pi^2(.076^2 + .060^2 + .069^2)/3$$

Anisotropic Equivalent to the Isotropic Temperature Factor

Sometimes we may only know the isotropic temperature factor and may want an estimate of the anisotropic matrix. For instance, in a least squares refinement procedure one often refines for the isotropic case first and then expands to the anisotropic. Starting parameters may be needed.

Define $\bar{\beta}$ as our estimated anisotropic matrix. Then from Equation 4

$$\frac{3}{4}B = tr(\bar{\beta}G)$$

We want $\bar{\beta}G = B/4I$ since the ellipse is constrained to a sphere in this case. Hence

$$\bar{\beta} = \frac{B}{4}G^*.$$

For the Si1 atom in coesite

$$\bar{\beta} = \frac{B}{4}G^*$$
$$= \frac{.37267}{4}\begin{bmatrix} .02636 & .00000 & .01324 \\ .00000 & .00654 & .00000 \\ .01324 & .00000 & .02608 \end{bmatrix}$$
$$= \begin{bmatrix} .00246 & .00000 & .00123 \\ .00000 & .00061 & .00000 \\ .01324 & .00000 & .00243 \end{bmatrix}$$
$$\text{observed } \beta - \bar{\beta} = \begin{bmatrix} .00022 & -.00027 & .00011 \\ -.00027 & -.00006 & -.00018 \\ .00011 & -.00018 & .00006 \end{bmatrix}.$$

As you can see, we get a pretty good estimate of the observed β from this method.

REFERENCES

Abramowitz, M. and Stegun, I.A. (1975) Handbook of mathematical functions. Dover Publications, Inc., New York, New York.

Alberti, A., Davoli, P. and Vezzalini, G. (1986) The crystal structure refinement of a natural mordenite. Zeitschrift für Kristallographie, 175, 249-256.

Alberti, A. and Sabelli, C. (1987) Statistical and true symmetry of ferrierite: possible absence of straight T-O-T bridging bonds. Zeitschrift für Kristallographie, 178, 249-256.

Angel, R. (1988) Crystal data for anorthites. Personal communication, Carnegie Institution of Washington.

Araki, T. (1980) Crystal structure of a cesium aluminosilicate, $Cs[AlSi_5O_{12}]$. Zeitschrift für Kristallographie, 152, 207-213.

Armbruster, T. (1986) Role of Na in the structure of low-cordierite: A single-crystal X-ray study. American Mineralogist, 71, 746-757.

Armbruster, T. (1986) Crystal structure refinement and thermal expansion of a Li, Na, Be-cordierite between 100 and 550 K. Zeitschrift für Kristallographie, 174, 205-217.

Armbruster, T., Bürgi, H.B., Kunz, M., Gnos, E., Brönnimann, S. and Lienert, C. (1990) Variation of displacement parameters in structure refinements of low albite. American Mineralogist, 75, 135-140.

Armbruster, T. and Oberhänsli, R. (1988) Crystal chemistry of double-ring silicates: Structural, chemical and optical variations in osumilites. American Mineralogist, 73, 585-594.

Artioli, G., Rinaldi, R., Kvick, Å. and Smith, J.V. (1986) Neutron diffraction structure refinement of the zeolite gismondine at 15 K. Zeolites, 6, 361-366.

Artioli, G., Smith, J.V. and Kvick, Å. (1984) Neutron diffraction study of Natrolite, $Na_2Al_2\ Si_3O_{10}\cdot 2H_2O$, at 20 K. Acta Crystallographia, C40, 1658-1662.

Artioli, G., Smith, J.V. and Pluth, J.J. (1986) X-ray structure refinement of mesolite. Acta Crystallographia, C42, 937-942.

Baur, W.H. (1971) The prediction of bond length variations in silicon-oxygen bonds. American Mineralogist, 56, 1573-1599.

Baur, W.H. (1977) Silicon-oxygen bond lengths, bridging angles Si-O-Si and synthetic low tridymite. Acta Crystallographia, B33, 2615-2619.

Baur, W.H. and Ohta T. (1982) The Si_5O_{16} pentamer in zunyite refined and empirical relations for individual silicon-oxygen bonds. Acta Crystallographia, B38, 390-401.

Bissert, G. and Liebau, F. (1986) The crystal structure of a triclinic bikitaite,

$Li[AlSi_2O_6] \cdot H_2O$, with ordered Al/Si distribution. Neues Jahrbuch für Mineralogie Monatshefte, 1986, 241-252.

Blasi, A., Brajkovic, A., De Pol Blasi, C., Foord, E.E., Martin, R.F. and Zanazzi, P.F. (1984) Structure refinement and genetic aspects of a microcline overgrowth on amazonite from Pikes Peak batholith, Colorado, U.S.A.. Bulletin de Minéralogie, 107, 411-422.

Blasi, A., De Pol Blasi, C. and Zanazzi, P.F. (1981) Structural study of a complex microperthite from anatexites at Mt. Caval, Argentera Massif, Maritime Alps. Neues Jahrbuch für Mineralogie Abhandlungen, 142, 71-90.

Blasi, A., De Pol Blasi, C. and Zanazzi, P.F. (1987) A re-examination of the Pellotsalo microcline: mineralogical implications and genetic considerations. Canadian Mineralogist, 25, 527-537.

Boisen, M.B., Jr. and Gibbs, G.V. (1985) Mathematical Crystallography, Volume 16, Reviews in Mineralogy. Mineralogical Society of America, Washington D.C..

Boisen, M. B., Jr., Gibbs, G. V., Downs, R. T. and D'Arco, P. (1990) The dependence of the SiO bond length on structural parameters in coesite, the silica polymorphs and the clathrasils. American Mineralogist, accepted, in press.

Bürgi, H.B. (1984) Stereochemical lability in crystalline coordination compounds. Transactions of the American Crystallographic Association, 20, 61-71.

Bürgi, H.B. (1989) Interpretation of atomic displacement parameters: Intramolecular translational oscillation and rigid-body motion. Acta Crystallographia, B45, 383-390.

Burnham, C.W., Ohashi, Y., Hafner, S.S. and Virgo, D. (1971) Cation distribution and atomic thermal vibrations in a iron-rich orthopyroxene. American Mineralogist, 56, 850-876.

Busing, W.R. and Levy, H.A. (1958) Determination of the principal axes of the anisotropic temperature factor. Acta Crystallographia, 11, 450-451.

Busing, W.R. and Levy, H.A. (1964) The effect of thermal motion on the estimation of bond lengths from diffraction measurements. Acta Crystallographia, 17, 142-146.

Busing, W.R., Martin, K.O. and Levy, H.A. (1964) ORFFE, a fortran function and error program. ORNL-TM-306, Oak Ridge National Laboratory.

Calestani, G., Bacca, G. and Andreetti, G.D. (1987) Structural study of zeolite X exchanged with 'f' transition elements. I. Crystal structure of reference hydrated Na-X. Zeolites, 7, 54-58.

Calligaris, M., Nardin, G., Randaccio, L. and Zangrando, E. (1986) Crystal structures of the hydrated and partially dehydrated forms of Cd-X exchanged zeolites. Zeolites, 6, 439-444.

Carpenter, G.B. (1969) Principles of crystal structure determination. W.A. Benjamin, Inc., New York, New York.

Chiari, G., Calleri, M., Bruno, E. and Ribbe, P.H. (1975) The structure of partially disordered synthetic strontium feldspar. American Mineralogist, 60, 111-119.

Cohen, J.P., Ross, F.K. and Gibbs, G.V. (1977) An X-ray and neutron diffraction study of hydrous low cordierite. American Mineralogist, 62, 67-78.

Cruickshank, D.W.J. (1956) The analysis of the anisotropic thermal motion of molecules in crystals. Acta Crystallographia, 9, 754-756.

Cruickshank, D.W.J. (1961) The role of *3d*-orbitals in π-bonds between (a) silicon, phosphorus, sulfur, or chlorine and (b) oxygen or nitrogen. The Journal of the Chemical Society, 1077, 5486-5504.

Czank, M. (1973) Strukturuntersuchungen von anorthit in temperaturbereich von 20° C bis 1430° C. Dissertation, Eidgenössischen Technischen Hochschule, Zürich.

Dollase, W.A. (1967) The crystal structure at 220° C of orthorhombic high tridymite from the Steinbach Meteorite. Acta Crystallographia, 23, 617-623.

Dunitz, J.D. (1985) From crystal statistics towards molecular dynamics. Transactions of the American Crystallographic Association, 20, 1-14.

Dunitz, J.D., Schomaker, V. and Trueblood, K.N. (1988) Interpretation of atomic displacement parameters from diffraction studies of crystals. The Journal of Physical Chemistry, 92, 856-867.

Feynman, R.P., Leighton, R.B. and Sands, M. (1977) The Feynman lectures on physics. Addison-Wesley Publishing Company, Reading, Massachusetts.

Flörke, O.W. (1954) Die ursachen der hoch-tief-umwandlungsanomalie von tridymit und cristobalit. Naturwiss., 41, 371-372.

Flörke, O.W. (1955) Strukturanomalien bei tridymit und cristobalit. Ber. Dt. Keram. Ges., 32, 369-381.

Franklin, J.N. (1968) Matrix Theory. Prentice-Hall, Inc., Englewood Cliffs, New Jersey.

Frondel, C. (1962) The System of Mineralogy, vol. 3, Silica Minerals. John Wiley and Sons, New York.

Galli, E. (1976) Crystal structure refinement of edingtonite. Acta Crystallographia, B32, 1623-1627.

Galli, E. and Alberti, A. (1975) The crystal structure of stellerite. Bulletin de la Société française de Minéralogie et de Cristallographie, 98, 11-18.

Geisinger, K.L., Spackman, M.A. and Gibbs, G.V. (1987) Exploration of structure, electron density distribution and bonding in coesite with Fourier and pseudoatom refinement methods using single-crystal X-ray diffraction data.

The Journal of Physical Chemistry, 91, 3237-3244.

Gerke, H. and Gies, H. (1984) Studies on clathrasils. IV: Crystal structure of dodecasil 1H, a synthetic clathrate compound of silica. Zeitschrift für Kristallographie, 166, 11-22.

Ghose, S., Schomaker, V. and McMullan, R.K. (1986) Enstatite, $Mg_2Si_2O_6$: A neutron diffraction refinement of the crystal structure and a rigid-body analysis of the thermal vibration. Zeitschrift für Kristallographie, 176, 159-175.

Gibbs, G.V., Hamil, M.M., Louisnathan, S.J., Bartell, L.S. and Yow, H. (1972) Correlations between Si-O bond length, Si-O-Si angle and bond overlap populations calculated using extended Hückel molecular orbital theory. American Mineralogist, 57, 1578-1613.

Gibbs, G.V., Prewitt, C.T. and Baldwin, K.J. (1977) A study of the structural chemistry of coesite. Zeitschrift für Kristallographie, 145, 108-123.

Gies, H. (1983) Studies on clathrasils. III. Crystal structure of melanophlogite, a natural clathrate compound of silica. Zeitschrift für Kristallographie, 164, 247-257.

Gies, H. (1984) Studies on clathrasils. VI. Crystal structure of dodecasil 3C, another synthetic clathrate compound of silica. Zeitschrift für Kristallographie, 167, 73-82.

Gies, H. (1986) Studies on clathrasils. IX. Crystal structure of deca-dodecasil 3R, the missing link between zeolites and clathrasils. Zeitschrift für Kristallographie, 175, 93-104.

Gramlich-Meier, R., Gramlich, V. and Meier, W.M. (1985) The crystal structure of the monoclinic variety of ferrierite. American Mineralogist, 70, 619-623.

Gramlich-Meier, R., Meier, W.M. and Smith, B.K. (1984) On faults in the framework structure of the zeolite ferrierite. Zeitschrift für Kristallographie, 169, 201-210.

Griffen, D.T. and Ribbe, P.H. (1976) Refinement of the crystal structure of celsian. American Mineralogist, 61, 414-418.

Griffen, D.T., Ribbe, P.H. and Gibbs, G.V. (1977) The structure of slawsonite, a strontium analog of paracelsian. American Mineralogist, 62, 31-35.

Grundy, H.D. and Ito, J. (1974) The refinement of the crystal structure of a synthetic non-stoichiometric Sr feldspar. American Mineralogist, 59, 1319-1326.

Hamilton, W.C. (1959) On the isotropic temperature factor equivalent to a given anisotropic temperature factor. Acta Crystallographia, 12, 609-610.

Hamilton, W.C. and Abrahams, S.C. (1970) International Union of Crystallography Commission on crystallographic apparatus: single-crystal intensity measurement project report II. Least-squares refinements of structural parameters.

Acta Crystallographia, A26, 18-24.

Harlow, G.E. and Brown, G.E., Jr. (1980) Low albite: an X-ray and neutron diffraction study. American Mineralogist, 65, 986-995.

Hill, R.J. and Gibbs, G.V. (1979) Variation in $d(T-\mathrm{O}), d(T\cdots T)$ and $\angle TOT$ in silica and silicate minerals, phosphates and aluminates. Acta Crystallographia, B35, 25-30.

Hirshfeld, F.L. (1976) Can X-ray data distinguish bonding effects from vibrational smearing. Acta Crystallographia, A32, 239-244.

Hochella, M.F., Jr., Brown, G.E., Jr., Ross, F.K. and Gibbs, G.V. (1979) High-temperature crystal chemistry of hydrous Mg- and Fe-cordierites. American Mineralogist, 64, 337-351.

Joswig, W., Bartl, H. and Fuess, H. (1984) Structure refinement of scolecite by neutron diffraction. Zeitschrift für Kristallographie, 166, 219-223.

Kalus, C. (1978) Neue strukturbestimmung des anorthits unter berocksichtigung möglicher alternativen. Dissertation, Ludwig-Maximilians-universität zu München.

Kato, K. and Nukui, A. (1976) Die kristallstruktur des monoklinen tief-tridymits. Acta Crystallographia, B32, 2486-2491.

Keefer, K.D. and Brown, G.E. (1978) Crystal structures and compositions of sanidine and high albite in cryptoperthitic intergrowth. American Mineralogist, 63, 1264-1273.

Kihara, K. (1977) An orthorhombic superstructure of tridymite existing between about 105 and 180° C. Zeitschrift für Kristallographie, 146, 185-203.

Kihara, K. (1978) Thermal change in unit-cell dimensions and a hexagonal structure of tridymite. Zeitschrift für Kristallographie, 148, 237-253.

Kihara, K., Matsumato, T. and Imamura, M. (1986a) Structural change of orthorhombic-I tridymite with temperature: a study based on second-order thermal -vibrational parameters. Zeitschrift für Kristallographie, 177, 27-38.

Kihara, K., Matsumato, T. and Imamura, M. (1986b) High-order thermal-motion tensor analyses of tridymite. Zeitschrift für Kristallographie, 177, 39-52.

Kirfel, A. and Will, G. (1984) Ending the "$P2_1/a$ coesite" discussion. Zeitschrift für Kristallographie, 167, 287-291.

Kirfel, A., Will, G. and Arndt, J. (1979) A new phase of coesite SiO_2. Zeitschrift für Kristallographie, 149, 315-326.

Klaska, R. and Jarchow, O. (1975) Die kristallstruktur und die verzwillingung von $RbAlSiO_4$. Zeitschrift für Kristallographie, 142, 225-238.

Konnert, J.H. and Appleman, D.E. (1978) The crystal structure of low tridymite. Acta Crystallographia, B34, 391-403.

Koyama, K. and Takéuchi, Y. (1977) Clinoptilolite: the distribution of potassium atoms and its role in thermal stability. Zeitschrift für Kristallographie, 145, 216-239.

Kunz, M. and Armbruster, T. (1990) Difference displacement parameters in alkali feldspars: Effect of (Si,Al) order-disorder. American Mineralogist, 75, 141-149.

Kvick, Å., Artioli, G. and Smith, J.V. (1986) Neutron diffraction study of the zeolite yugawaralite at 13 K. Zeitschrift für Kristallographie, 174, 265-281.

Kvick, Å. and Smith, J.V. (1983) A neutron diffraction study of the zeolite edingtonite. The Journal of Chemical Physics, 79, 2356-2362.

Kvick, Å., Ståhl, K. and Smith, J.V. (1985) A neutron diffraction study of the bonding of zeolitic water in scolecite at 20 K. Zeitschrift für Kristallographie, 171, 141-154.

Lager, G.A., Jorgensen, J.D. and Rotella, F.J. (1982) Crystal structure and thermal expansion of α-quartz SiO_2 at low temperatures. The Journal of Applied Physics, 53, 6751-6756.

Le Page, Y. and Donnay G. (1976) Refinement of the crystal structure of low-quartz. Acta Crystallographia, B32, 2456-2459.

Levien, L. and Prewitt, C.T. (1981) High-pressure crystal structure and compressibility of coesite. American Mineralogist, 66, 324-333.

Levien, L., Prewitt, C.T. and Weidner, D.J. (1980) Structure and elastic properties of quartz at pressure. American Mineralogist, 65, 920-930.

Liebau, F. (1985) Structural chemistry of silicates: structure, bonding and classification. Springer-Verlag, Berlin.

Lipson, H. and Cochran, W (1953) The determination of crystal structures. G. Bell and Sons Ltd., London, England.

Mazzi, F., Galli, E. and Gottardi, G. (1984) Crystal structure refinement of two tetragonal edingtonites. Neues Jahrbuch für Mineralogie Monatshefte, 1984, 373-382.

Megaw, H.D. (1974) The architecture of the feldspars. In The Feldspars, editors W.S. MacKenzie and J. Zussman. Manchester University Press, Manchester, England.

Mortier, W.J., Pluth, J.J. and Smith, J.V. (1976) The crystal structure of dehydrated natural offretite with stacking faults of erionite type. Zeitschrift für Kristallographie, 143, 319-332.

Mortier, W.J., Pluth, J.J. and Smith, J.V. (1976) Crystal structure of natural zeolite offretite after carbon monoxide adsorption. Zeitschrift für Kristallographie, 144, 32-41.

Nelmes, R.J. (1969) Representational surfaces for thermal motion. Acta Crystallographia, A25, 523-526.

Newton, M.D. and Gibbs, G.V. (1980) *Ab initio* calculated geometries and charge distributions for H_4SiO_4 and $H_6Si_2O_7$ compared with experimental values for silicates and siloxanes. Physics and Chemistry of Minerals, 6, 221-246.

Novak, G.A. and Gibbs, G.V. (1971) The crystal chemistry of the silicate garnets. American Mineralogist, 56, 791-825.

Peacor, D.R. (1973) High-temperature single-crystal study of the cristobalite inversion. Zeitschrift für Kristallographie, 138, 274-298.

Pechar, F. (1988) The crystal structure of natural monoclinic analcime ($NaAlSi_2O_6 \cdot H_2O$). Zeitschrift für Kristallographie, 184, 63-69.

Peterse, W.J.A.M. and Palm, J.H. (1966) The anisotropic temperature factor of atoms in special positions. Acta Crystallographia, 20, 147-150.

Phillips, M.W. and Ribbe, P.H. (1973) The structures of monoclinic potassium-rich feldspars. American Mineralogist, 58, 263-270.

Phillips, M.W., Ribbe, P.H. and Pinkerton, A.A. (1989) The structure of intermediate albite, $NaAlSi_3O_8$. Acta Crystallographia, C45, 542-545.

Pluth, J.J., Smith, J.V. and Faber, J., Jr. (1985) Crystal structure of low cristobalite at 10, 293 and 473 K: Variation of framework geometry with temperature. The Journal of Applied Physics, 57, 1045-1049.

Pluth, J.J., Smith, J.V. and Kvick, Å. (1985) Neutron diffraction study of the zeolite thomsonite. Zeolites, 5, 74-80.

Prince, E., Donnay, G. and Martin, R.F. (1973) Neutron diffraction refinement of an ordered orthoclase structure. American Mineralogist, 58, 500-507.

Rouse, R.C. and Peacor, D.R. (1986) Crystal structure of the zeolite mineral goosecreekite, $CaAl_2Si_6O_{16} \cdot 5H_2O$. American Mineralogist, 71, 1494-1501.

Sahl, K. (1980) Refinement of the crystal structure of bicchulite, $Ca_2\ [Al_2SiO_6]\ (OH)_2$. Zeitschrift für Kristallographie, 152, 13-21.

Scambos, T.A., Smyth, J.R. and McCormick, T.C. (1987) Crystal-structure refinement of high sanidine from the upper mantle. American Mineralogist, 72, 973-978.

Schlenker, J.L., Pluth, J.J. and Smith, J.V. (1977) Refinement of the crystal structure of brewsterite, $Ba_{0.5}Sr_{1.5}Al_4Si_{12}O_{32} \cdot 10H_2O$. Acta Crystallographia, B33, 2907-2910.

Schulz, H. (1972) Influence of "split" atoms on anisotropic temperature factors (shown at the example of quartz-like silicates of composition $Li_2O \cdot Al_2O_3 \cdot xSiO_2$ with $x \geq 2$). Zeitschrift für Kristallographie, 136, 321-349.

Smith, G.S. and Alexander, L.E. (1963) Refinement of the atomic parameters of α-quartz. Acta Crystallographia, 16, 462-471.

Smith, J.V. (1954) A review of the Al-O and Si-O distances. Acta Crystallographia, 7, 479-481.

Smith, J.V. and Bailey, S.W. (1963) Second review of Al-O and Si-O tetrahedral distances. Acta Crystallographia, 16, 801-811.

Smith, J.V., Artioli, G. and Kvick, Å. (1986) Low albite, $NaAlSi_3O_8$: Neutron diffraction study of crystal structure at 13 K. American Mineralogist, 71, 727-733.

Smyth, J.R., Smith, J.V., Artioli, G. and Kvick, Å. (1987) Crystal structure of coesite, a high-pressure form of SiO_2, at 15 and 298K from single-crystal neutron and X-ray diffraction data: test of bonding models. The Journal of Physical Chemistry, 91, 988-992.

Strob, W.D. (1981) Strukturverfeinerung eines tief-mikroklins, zusammenhänge zwischen $\langle T-O \rangle$ abständen und Al, Si- ordnungsgrad und metrische variation in einer tief-albit/tief-mikroklin - mischkristallreiche. Dissertation, Westfälischen Wilhelms-Universität, Münster.

Tagai, T., Joswig, W. and Korekawa, M (1980) Die bestimmung der Al/Si-verteilung mittels neutronenbeugung in einem plagioklas An_{66}. Zeitschrift für Kristallographie, 151, 77-89.

Thöni, W. (1975) The crystal structure of hydrated zeolites Tl-*A*, Ca-*A* and Ag-*A*. Zeitschrift für Kristallographie, 142, 142-160.

Tscherry, V., Schulz, H. and Laves, F. (1972) Average and super structure of β eucryptite ($LiAlSiO_4$) Part I. Average structure. Zeitschrift für Kristallographie, 135, 161-174.

Vaughan, P.A. (1966) The crystal structure of the zeolite ferrierite. Acta Crystallographia, 21, 983-990.

Wallace, J.H. and Wenk, H.R. (1980) Structural variation in low cordierites. American Mineralogist, 65, 96-111.

Waser, J. (1955) The anisotropic temperature factor in triclinic coordinates. Acta Crystallographia, 8, 731.

Weitz, G. (1972) Die struktur des sanidins bei verschiedenen ordnungsgraden. Zeitschrift für Kristallographie, 136, 418-426.

Wenk, H.R. and Kroll, H. (1984) Analysis of $P\bar{1}$, $I\bar{1}$ and $C\bar{1}$ plagioclase structures. Bulletin de Minéralogie, 107, 467-487.

Willis, B.T.M. and Pryor, A.W. (1975) Thermal vibrations in crystallography. Cambridge University Press, Cambridge, England.

Winter, J.K., Ghose, S. and Okamura, F.P. (1977) A high-temperature study of

the thermal expansion and the anisotropy of the sodium atom in low albite. American Mineralogist, 62, 921-931.

Winter, J.K., Okamura, F.P. and Ghose, S. (1979) A high-temperature structural study of the high albite, monalbite and the analbite→ monalbite phase transition. American Mineralogist, 64, 409-423.

Wright, A.F. and Lehmann, M.S. (1981) The structure of quartz at 25 and 590° C determined by neutron diffraction. The Journal of Solid State Chemistry, 36, 371-380.

Young, R.A. and Post, B. (1962) Electron density and thermal effects in alpha quartz. Acta Crystallographia, 15, 337-346.

Zachariasen, W.H. (1969) Concluding remarks. Acta Crystallographia, A25, 276.

Zachariasen, W.H. and Plettinger, H.A. (1965) Extinction in quartz. Acta Crystallographia, 18, 710-714.

The vita has been removed from the scanned document